UNIVERSIDADE D
COIMBRA

Filipe Miguel Martins Macedo Serrano Coelho

Evaporação de Hawking e instabilidades superradiantes de buracos negros primordiais no axiverso da teoria de cordas

Dissertação no âmbito do Mestrado em Física, ramo Física Nuclear e de Partículas orientada pelo Professor Doutor João Pedro Trancoso Gomes Rosa e apresentada ao Departamento de Física da Faculdade de Ciências e Tecnologia da Universidade de Coimbra

setembro de 2022

Hawking evaporation and superradiant instabilities of primordial black holes in the axiverse of string theory

1 2 9 0

UNIVERSIDADE D
COIMBRA

Filipe Coelho

September 20, 2022

Abstract-Resumo

From Kaluza-Klein compactifications of string theory, a large number of Axion-Like-Particles (ALPs) emerge as zero modes of p-forms such as the Ramond-Ramond fields. We present a mechanism in which a rotating Primordial Black Hole, which is evaporating today, can be used to measure the amount of light ALP species present in the axiverse and dynamically trigger a superradiant instability of a heavy ALP whose mass can be unequivocally measured directly from the properties of the Black Hole.

Keywords— Primordial Black Hole, Hawking Evaporation, Superradiance

Das compactificações Kaluza-Klein da teoria de cordas, um grande número de Axion-Like-Particles (ALPs) emerge como modos zero de p-formas, tais como os campos Ramond-Ramond. Apresentamos um mecanismo em que um Buraco Negro Primordial com rotação, que se está a evaporar atualmente, pode ser utilizado para medir a quantidade de espécies de ALPs leves presentes no axiverso e desencadear dinamicamente uma instabilidade superradiante de um ALP pesado cuja massa pode ser inequivocamente medida directamente a partir das propriedades do Buraco Negro.

Palavras-Chave— Buraco Negro Primordial, Evaporação de Hawking, Superradiância

Dedication

To my mother, my grandmother and my girlfriend

Acknowledgements

I want to thank FCT, for supporting this work through the project "Evaporação e instabilidades superradiantes de buracos negros primordiais no axiverso da teoria de cordas", (UIBD/04564/2020).

I also want to thank Dr. João Rosa for the help and the extremely important life lessons that I will cherish for the rest of my career, and thank PhD student Marco Calzà for the valuable insights and discussions.

Finally, I want to thank my mother, my grandmother, my girlfriend, and my friends for listening to my endless and tedious talks about physics, and for always supporting me.

Contents

Preface

In this thesis I review the work done in the last year under the supervision of Professor João Rosa with the helpful insights from PhD student Marco Calzà. The main topic is black hole dynamics, namely superradiant instabilities and Hawking radiation, in a universe with a large number of light scalar particles added to the Standard Model. This topic is motivated by String Theory, where a large number of scalar fields is predicted as a result of Kaluza-Klein compactifications of extra dimensions, giving rise to the *String Axiverse*. In order to maximize the radiative effects from Hawking radiation, we also considered the study of the dynamics of very light Black Holes, namely with masses of 10^{12} kg, which are not created by stellar collapse, but by density fluctuations in the early universe - *Primordial Black Holes*.

Although the phenomenology proposed is extremely interesting and has fascinating physical consequences, this thesis focuses more on the mathematical structure and the formalism used to determine the dynamics of the system. With this in mind, the first chapter is a review of the mathematical theory of Black Holes and functions as a "root structure" which ramifies to both effects (superradiance and Hawking radiation) in chapter 2. These will be discussed thoroughly and finally two sections will be dedicated to Primordial Black Holes and the String Axiverse for contextualization. Chapter 1 and 2 are then purely review of literature on these topics.

Afterwards, we proceed to the actual work done. Chapter 3 describes a toy model of the universe, where only 2 types of particles are being considered. A

massless scalar field, which is being emitted through Hawking radiation, and a 1 GeV scalar field, which induces a superradiant instability. Although Hawking radiation with a massless scalar and superradiant instabilities with a massive scalar are known individually, the dynamically triggered instability through Hawking evaporation shown in the final section of that chapter is new work.

In chapter 4, we improve on the work done in the previous chapter considering the Standard Model plus a large number of scalar fields being emitted through Hawking radiation and, again, dynamically trigger an instability of a massive scalar field. The superradiant part comes as an addition to a previous work done by Rosa, Calzà and March-Russell [1], and is also new work.

Finally, we discuss future work and possible considerations in chapter 5.

Notation and Conventions

Throughout this thesis I will use Planck units ($\hbar = c = G = 1$) to write down every equation used but all plots and initial conditions will be in SI units for the properties of the Black Hole. Every particle physics notion will be in Natural units for an easier grasp of the orders of magnitude shown here. I will use metric signature $(- + + +)$ so that spacelike hypersurfaces have positive norm. I will also use *abstract index notation*, introduced by Roger Penrose [2] meaning my indices will not be numerical, but only serve to denote the characteristics of the tensor (e.g. g_{ab} is a two-tensor). Spacetime tensor indices will be denoted by lower case roman letters while spinorial indices will be denoted by upper case Roman letters. Also every numerical computation was independently computed in both Python and Wolfram Mathematica [3], and only results that were equivalent (with no precise definition of equivalent defined in this context) are given in this thesis. Finally I will denote complex conjugation by a bar on top of the function (e.g. $\bar{i} = -i$, $i^2 = -1$).

Acronyms

ALP Axion Like Particle. 34

DOF Degrees of Freedom. 21

EOM Equations Of Motion. 17

HE Hawking Evaporation. 26

KK Kaluza-Klein. 33

NEC Null Energy Condition. 11

NP Newman-Penrose. 7

PBH Primordial Black Hole. 31

QCD Quantum Chromodynamics. 32

QFT Quantum Field Theory. 12

SEC Strong Energy Condition. 11

SR Superradiance. 17

WEC Weak Energy Condition. 11

Nomenclature

$\hbar$	Reduced Planck's constant
c	Speed of light
G	Universal gravitational constant
R_{ab}	Ricci tensor
V_x	Tangent Space at x
R	Ricci scalar
T_{ab}	Energy-momentum tensor
$\pounds_\chi$	Lie derivative with respect to the Killing field χ^a
$I^\pm(S)$	Chronological future/past of the set S
$J^\pm(S)$	Causal future/past of the set S
$D^\pm(S)$	Future/past domain of dependence of the closed, achronal set S
$\mathscr{I}^\pm$	Future/past null infinity
i^0	Spatial infinity
$i^\pm$	Future/past timelike infinity

All causal structure and assymptotical flatness definitions are taken from [4].

List of Figures

List of Tables

Chapter 1

General Relativity

In this chapter, I aim to introduce the theory and the mathematical tools used in order to understand black holes, their properties, and the necessary theorems needed to correctly describe the phenomenology proposed in this thesis.

In section 1.1, I will introduce the Einstein Field Equations and the Schwarzchild spacetime, the simplest black hole solution.

Later, I will define rigorously what a black hole is, and what is needed to fully characterize its dynamics in section 1.2.

In section 1.3, I will introduce the Kerr spacetime and understand the different physically possible regimes as well as the degrees of freedom of the theory.

After introducing the metric I will discuss the mathematical formalism used when describing particle physics. This is the Newman-Penrose formalism that will be employed to facilitate the work done in the last chapters, which can be greatly simplified by using the symmetries of the Kerr metric in a more "hands-on" fashion. This will be in section 1.4.

Afterward, in section 1.5, I will return to the study of black holes and explore the Area theorem, which will be introduced alongside all important assumptions and their importance to the theorem.

Finally, a review of black hole Thermodynamics will be presented in section 1.6, motivating the interpretation of the surface gravity of a Black hole as its tem-

perature. A result that shall be understood in chapter 2.

1.1 Introduction

General Relativity is one of the most famous theories ever created. Its formulation, in 1915, allowed us to predict some of the most fascinating concepts known to man. In particular, it allowed us to predict the unavoidable death of a star and conjure the idea that a star can be so massive that, at the end of its lifetime, the gravitational collapse results in a space-time singularity [5]. This process leads to the creation of a black hole, but it is not the only way. Indeed, black hole solutions appear very naturally in Einstein's equations

$$R_{ab} - \frac{1}{2}Rg_{ab} = 8\pi T_{ab} \tag{1.1}$$

where R_{ab} is the Ricci tensor, R is the Ricci scalar, g_{ab} is the metric tensor and T_{ab} is the energy-momentum tensor. Symmetry conditions in this equation lead to precise analytical solutions and the most famous ones in vacuum, $R_{ab} = 0$, show how black holes, truly are geometrical deformities of spacetime itself. For instance, considering a spacetime (M, g_{ab}) which is *spherically symmetric*, i.e., admits the group $SO(3)$ as the group of isometries, with those group orbits being spacelike two-surfaces [4]. Through Birkhoff's Theorem [6], the vacuum solution must also be asymptotically flat and *static*, i.e., admits a one parameter group of isometries whose orbits are timelike curves (this describes *stationarity*) and also posses a "time reflection" symmetry [4]. This solution is, of course, given by the Schwarzchild metric

$$ds^2 = -\left(1 - \frac{2M}{r}\right)dt^2 + \left(1 - \frac{2M}{r}\right)^{-1}dr^2 + r^2 d\Omega^2 \tag{1.2}$$

Since this is a static solution, it does not accurately represent a black hole formed due to matter collapse. Nevertheless, it can be extremely useful to provide an insight into the basic properties of black holes. This is because, at late times, we expect the metric of a physical black hole to converge to the Schwarzchild case (I will return to this later).

1.2 Black holes

Before proceeding, it is important to precisely define what a black hole is in a strongly asymptotically predictable and flat spacetime (these are the spacetimes I will study, and very crudely means that they are Minkowski for large distances and possess no naked singularities [4]). The necessity for asymptotic flatness comes from the fact that an asymptotic observer is causally disconnected from the black hole, hence we can define a black hole, B, as being the difference between the manifold, M, and the causal past of the future null infinity ($B = M - J^-(\mathscr{I}^+)$), since $\mathscr{I}^+$ contains the information that can reach an asymptotic observer. The necessity for strong asymptotical predictableness comes from the fact that we want $J^-(\mathscr{I}^+)$ to be "well behaved"[1], but as a subset of the manifold while not being the manifold itself ($J^-(\mathscr{I}^+) \subset M \wedge J^-(\mathscr{I}^+) \neq M$). A black hole is now defined in a very simple way and its boundary, $H = \dot{J}^-(\mathscr{I}^+) \cap M$, is called the *event horizon*. On stationary asymptotically flat spacetimes, this null hypersurface is, by Hawking's theorem [6], a Killing Horizon, which means it admits a Killing field, χ^a which is normal to H. It is then possible to characterize H completely by an invariant, κ, under transformations generated by χ^a

$$\pounds_\chi \kappa = 0 \tag{1.3}$$

The invariant κ is defined as a proportionality function

$$\nabla^a \left(\chi^b \chi_b\right) = -2\kappa\chi^a \tag{1.4}$$

and can be completely determined using Frobernius's theorem [4]

$$\chi_{[a}\nabla_b\chi_{c]} = 0 \tag{1.5}$$

giving the formula

$$\kappa^2 = -\frac{1}{2}\left(\nabla^a\chi^b\right)\left(\nabla_a\chi_b\right) \tag{1.6}$$

[1] Obeying properties like global hyperbolicity, which is defined in section (1.5).

where the evaluation at the horizon is implicit. This is a constant through and across orbits (up to a sign) of χ^a, which shows that its characterization suffices to completely understand the properties of the horizon. It has the physical interpretation of the *surface gravity* of the black hole, and as we shall see in section (2.2) contains information about the temperature of the black hole.

1.3 Kerr metric

Another very important example of a black hole solution and the one I will be more focused on in this thesis is the Kerr spacetime, which is a vacuum solution considering a *stationary*, and *axisymmetric* spacetime, i.e., a spacetime that admits a one-parameter group of isometries whose orbits are closed spacelike curves. This spacetime represents a rotating black hole and its metric, in the Boyer-Lindquist coordinates [7], is given by

$$\begin{aligned} ds^2 = &- \frac{\Delta - a^2 \sin^2\theta}{\Sigma} dt^2 - 2a \sin^2\theta \frac{r^2 + a^2 - \Delta}{\Sigma} dt d\varphi \\ &+ \left[\frac{\left(r^2 + a^2\right)^2 - \Delta a^2 \sin^2\theta}{\Sigma} \right] \sin^2 d\varphi^2 + \frac{\Sigma}{\Delta} dr^2 + \Sigma d\theta^2 \end{aligned} \tag{1.7}$$

where $\Sigma = r^2 + a^2 \cos^2\theta$ and $\Delta = r^2 + a^2 - 2Mr$. We identify M and a as the parameters of the theory and I will now demonstrate their relationship to the mass and angular momentum. The symmetries of the Kerr solution inform us of the existence of the timelike Killing field, $\xi^a = \partial_t^a$, and the axial Killing field, $\psi^a = \partial_\varphi^a$. Since this is an asymptotically flat spacetime and is a vacuum near infinity (it is indeed a vacuum everywhere), we can relate the physicality of the parameters M and a to the Killing vectors considering an arbitrary two-sphere, S, in the asymptotic region and integrating the two-form

$$M = -\frac{1}{8\pi} \int_S \epsilon_{abcd} \nabla^c \xi^d \tag{1.8}$$

allowing us to identify M as the mass of the black hole, and

$$Ma = -\frac{1}{16\pi}\int_S \epsilon_{abcd}\nabla^c\psi^d \tag{1.9}$$

confirming $aM = J$ to be the angular momentum of the black hole.

The inverse metric can be calculated through the cofactor metric and the determinant of the metric

$$g^{ab} = \frac{\mathrm{cof}\,(g_{ab})}{g} \tag{1.10}$$

where the determinant is $g = -\Sigma^2 \sin^2\theta$. The components of the inverse metric are then

$$g^{\mu\nu} = \begin{pmatrix} \frac{a^2\Delta\sin^2\theta-(r^2+a^2)^2}{\Delta\Sigma} & 0 & 0 & -\frac{a}{\Delta}\frac{r^2+a^2-\Delta}{\Sigma} \\ 0 & \frac{\Delta}{\Sigma} & 0 & 0 \\ 0 & 0 & \frac{1}{\Sigma} & 0 \\ -\frac{a}{\Delta}\frac{r^2+a^2-\Delta}{\Sigma} & 0 & 0 & \frac{\Delta-a^2\sin^2\theta}{\sin^2\theta\Delta\Sigma} \end{pmatrix} \tag{1.11}$$

We can see from looking at equations (1.7) and (1.11) that we have potential singularities at

$$\Delta = r^2 + a^2 - 2Mr = 0 \tag{1.12}$$

$$\Sigma = r^2 + a^2\cos^2\theta = 0 \tag{1.13}$$

We begin by studying the case $\Delta = 0$ giving the roots

$$r_\pm = M \pm \sqrt{M^2 - a^2} \tag{1.14}$$

We want to study the physical case in which $a < M$ [8]. I shall then introduce the *reduced* angular momentum, $\tilde{a}$, s.t.,

$$\tilde{a} = \frac{a}{M} < 1 \tag{1.15}$$

allowing us to write Eq (1.14) as

$$r_{\pm} = M\left(1 \pm \sqrt{1-\tilde{a}^2}\right) \tag{1.16}$$

These roots identify the inner and outer horizon and behave very much as the Schwarzchild horizon $r = 2M$, such that they are coordinate singularities. Per section (1.2), the horizon, H, coincides with the outer horizon, r_+. The roots of Σ define the *singularity ring* and present no physical importance to this thesis due to being causally disconnected to the asymptotic observer ($R \notin J^-(\mathscr{I}^+)$, with R denoting the singularity ring).

Another important fact about the Kerr spacetime is that the timelike Killing field ξ^a becomes spacelike in the region

$$r_+ < r < M\left(1 + \sqrt{1-\tilde{a}^2\cos^2\theta}\right) \tag{1.17}$$

This defines the *ergoregion* and imposes non-stationarity of observers within this region.

To finish this section, I shall briefly discuss the topology of the Horizon, H, in accord with the study made in the previous section. Since the Kerr metric is stationary and asymptotically flat, it admits a Killing vector χ^a normal to H. Since the Killing vectors constitute a closed algebra with the Lie derivative, χ^a must be a linear combination of ξ^a and ψ^a

$$\chi^a = \xi^a + \Omega_H \psi^a \tag{1.18}$$

where Ω_H is a normalization constant imposed by asymptotic flatness. Its value has the physical interpretation of the angular velocity of the black hole

$$\Omega_H = \left(\frac{d\varphi}{dt}\right)_{r=r_+} = -\left(\frac{g_{t\varphi}}{g_{\varphi\varphi}}\right)_{r=r_+} = \frac{a}{r_+^2 + a^2} = \frac{\tilde{a}}{2r_+} \tag{1.19}$$

and associated with this Killing horizon $H = r_+$ we have the value for the surface

gravity, κ, to be

$$\kappa = \frac{\sqrt{M^2 - a^2}}{2Mr_+} = \frac{\sqrt{1 - \tilde{a}^2}}{2r_+} \tag{1.20}$$

This concludes the analysis of the Kerr spacetime.

1.4 Newman-Penrose formalism

The symmetries of the Kerr spacetime allow us to have simple and separable equations for the different fields that we want to study. But when studying particle physics, one has to take into account the existence of a fermionic field which is not a natural object defined on a Lorentzian manifold. It is then wise to adopt a formalism in which fermions are treated similarly as one would treat a tensorial field. This formalism is known as the Newman-Penrose (NP) formalism. But before I introduce it, let us consider the general properties of spinors on general spacetimes to motivate the structure of the formalism.

A spinor is an extremely interesting object whose nature can only truly be understood in Minkowski spacetime. This is because the Minkowski spacetime admits the Lorentz group $O(3,1)$ as its group of isometries. And this group possesses a spinorial projective representation [9, 10]. This means that, considering 2 elements, Λ_1 and Λ_2, of $O(3,1)$, the product rule reads

$$U(\Lambda_1)U(\Lambda_2) = e^{i\phi}U(\Lambda_1\Lambda_2) \tag{1.21}$$

where $U(\Lambda)$ is a unitary representation of Λ, and $\phi = \phi(\Lambda_1, \Lambda_2)$ is a real function. Wigner showed that, for the Lorentz group, $e^{i\phi} = \pm 1$ (-1 for spinors) [9]. This shows how unnaturally spinors are defined in a spacetime. Considering that we could draw a spinor as an arrow in a spacetime, (M, g_{ab}), and considering a closed loop in $O(3,1)$, because of the minus sign in Eq. (1.21), the arrow would go to minus itself, thus proving, by *reductio ad absurdum*, that a spinor is not physical.

It is not until the homomorphism between $SL(2,\mathbb{C})$[2] and the *proper* Lorentz

[2] This is the group of linear maps of unit determinant of a complex two-dimensional vector space into itself.

group, $SO(3,1)$[3] is made that the physical interpretation of a spinor as a *Null flag* [2] is understood. Consider a spinor ψ^A defined in a two dimensional spinor space $(\mathcal{W}, \epsilon_{AB})$ (the *skew metric*, ϵ_{AB} works very much like the spacetime metric, g_{ab}, except that it is completely antisymmetric). We can construct the Null flag associated with the spinor ψ^A as

$$F^{AA'BB'} = \psi^A \psi^B \bar{\epsilon}^{A'B'} + \bar{\psi}^{A'} \bar{\psi}^{B'} \epsilon^{AB} \tag{1.22}$$

where primed indices represent elements of the dual complex space $\overline{\mathcal{W}}^*$. There is a one-to-one correspondence between null two-tensors and null flags,

$$F^{ab} = \sigma^a_{AA'} \sigma^b_{BB'} F^{AA'BB'} \tag{1.23}$$

for some non-degenerate $\sigma^a_{AA'}$. Two spinors, ψ^A and ξ^A, give rise to the same null flag if they differ by a sign, $\psi^A = \pm\xi^A$, which means this is the best physical interpretation of what a spinor is, and is the key to understanding how one constructs a formalism to work regardless of the representation used. Since the null flag can always be written as a difference between two orthogonal null vectors, we expect spinors to transform closely to a two-tensor and are led to take into account a basis of null vectors in Minkowski spacetime.

Let us now consider a *dyad* basis, o^A and l^A, for $\mathcal{W}$ satisfying $o_A l^A = 1$. We can write a basis of null vectors for Minkowski spacetime as

$$l^a = \sigma^a_{AA'} l^A \bar{l}^{A'} \tag{1.24}$$

$$n^a = \sigma^a_{AA'} o^A \bar{o}^{A'} \tag{1.25}$$

$$m^a = \sigma^a_{AA'} l^A \bar{o}^{A'} \tag{1.26}$$

$$\bar{m}^a = \sigma^a_{AA'} o^A \bar{l}^{A'} \tag{1.27}$$

We can then see that if one considers a basis for spinor space, we can get a basis of null vectors for Minkowski spacetime. But for this to hold in a general spacetime

[3] This is the set of Lorentz transformations with unit determinant.

(with some restrictions [2, 4]), we would need projective representations of $GL(4,\mathbb{R})$, which we do not. Nevertheless, we can still define a spinor individually at each Tangent Space, V_p, at each point, $p \in M$. But if one were to consider the group of isometries of the Tangent Space at each point as a local Lorentz group, one could create a map that relates the curved space metric, g_{ab} to the Minkowski metric of the Tangent Space, $\eta_{AA'BB'}$, at each point. Such a map is called a *vierbein*, $e_a^{AA'}$ and it is defined as a bilinear map that has both Minkoswkian and spacetime indices

$$\eta_{AA'BB'} e_a^{AA'} e_b^{BB'} = g_{ab} \tag{1.28}$$

$$e^{aAA'} = g^{ab} e_b^{AA'} \tag{1.29}$$

$$e^{aAA'} = \eta^{AA'BB'} e^a_{BB'} \tag{1.30}$$

where AA' are tensor indices in spinor space which we know are related to Minkowski indices. This way, we define a notion of a *local Lorentz frame* and consider the *vierbein* as a local basis for the Tangent Space. A *vierbein* formalism with null vectors generated by a dyad is called the **Newman-Penrose formalism**. Finally, to fully construct the formalism, one has to first identify the directional derivatives of the *vierbein*. These directional derivatives are called the *Ricci rotation coefficients*, $(\omega_{CC'AA'BB'})$, which, because of the null construction coming from spinor formalism, are also called *spin coefficients* in the Newman-Penrose formalism. They take the form

$$\omega_{CC'AA'BB'} = e^a_{CC'} \nabla_b e_{AA'a} e^b_{BB'} \tag{1.31}$$

and allow us to define the intrinsic derivative [11],

$$A_{AA'|BB'} = e^a_{AA'} \nabla_b A_a e^b_{BB'} = \partial_{BB'} A_{AA'} - \eta^{CC'DD'} \omega_{CC'AA'BB'} A_{DD'} \tag{1.32}$$

The goal is then to project every tensor onto these vectors and isolate the independent components using the symmetry of the spacetime.

Consider then the null *vierbein* $\{l^a, n^a, m^a, \bar{m}^a\}$. To be consistent with the

dyad introduced earlier,

$$l^a m_a = l^a \bar{m}_a = n^a m_a = n^a \bar{m}_a = 0 \tag{1.33}$$

$$l^a n_a = -1 \quad m^a \bar{m}_a = 1 \tag{1.34}$$

In this formalism, the directional derivatives are all independently named

$$D = l^a \partial_a \quad \Delta = n^a \partial_a \quad \delta = m^a \partial_a \quad \bar{\delta} = \bar{m}^a \partial_a \tag{1.35}$$

and so are the spin coefficients

$$\begin{aligned} \kappa &= \omega_{311} \quad \rho = \omega_{314} \quad \varepsilon = \frac{1}{2}(\omega_{211} + \omega_{341}) \\ \sigma &= \omega_{313} \quad \mu = \omega_{243} \quad \gamma = \frac{1}{2}(\omega_{212} + \omega_{342}) \\ \lambda &= \omega_{244} \quad \tau = \omega_{312} \quad \alpha = \frac{1}{2}(\omega_{214} + \omega_{344}) \\ \nu &= \omega_{242} \quad \pi = \omega_{241} \quad \beta = \frac{1}{2}(\omega_{213} + \omega_{343}) \end{aligned} \tag{1.36}$$

The potential symmetries of the spacetime become highly visible in this way because they are seen as zeros in some of the spin coefficients. Indeed, there is a one-to-one correspondence between the roots of different coefficients and the special algebraic classification, also known as the *Petrov classification* of the spacetime [11, 12]. This is because we can choose a null *vierbein*, *s.t.*, one of the vectors is aligned with one of the repeated principal null vectors[4], which make it so that various components of the Weyl tensor projected in the *vierbein* are null, which also imposes that certain spin coefficients are null. This will be very important in the next chapter where we shall use this formalism to discuss the Teukolsky equation, *s.t.*, we can describe Hawking Evaporation of all the different matter fields consistently and in a simple manner.

[4] These are null vectors which are *eigenvectors* of the Weyl tensor with null norm and satisfy different equations based on how many of these vectors are repeated [4].

1.5 Area Theorem

Continuing the study of black holes, it would not be wise to leave this chapter without discussing first the Area theorem proposed by Hawking [13]. The reason for this is that both Superradiance and Hawking Evaporation have a simple and quite beautiful relationship to it, and so I decided to dedicate this section to stating the theorem, understanding every notion required for it (besides strong asymptotical predictability in order to avoid a chain of theorems) and comprehending their necessity. I shall begin this analysis by first considering a causal structure notion, that of a *Cauchy Surface*, Σ. This is a closed achronal ($I^+(\Sigma) \cap \Sigma = \emptyset$) that has the entire manifold as its Cauchy development, $D(\Sigma) = M$. A spacetime, (M, g_{ab}), that contains said surface is said to be *globally hyperbolic*. Its importance comes in the fact that a Cauchy surface constitutes an instant of time and is the adequate surface to identify important notions such as a black hole at an instant of time, $\mathscr{B} = B \cap \Sigma$, or even the dot product on a quantum field at a certain time (I will return to this in section 2.2). This is because any event at a point $p \in M$ has to have been registered at Σ (in the case where $p \in D^+(\Sigma)$), which means that we can use the initial data in Σ to predict the entire past and future of a classical theory on a globally hyperbolic spacetime.

Another important concept, which is crucial for the area theorem, is the *Null Energy Condition (NEC)* which states that for any null vector k^a, $T_{ab}k^ak^b \geq 0$. We can trivially derive the geometric version of this concept using Eq. (1.1) to write $R_{ab}k^ak^b \geq 0$, which is also usually called the *Null Convergence Condition* [6]. Unlike the *Weak Energy Condition (WEC)*, which has the form $T_{ab}\xi^a\xi^b \geq 0$, for all timelike ξ^a, and the *Strong Energy Condition (SEC)*, which has the geometric form $R_{ab}\xi^a\xi^b \geq 0$, for all timelike ξ^a, the physical interpretation of the NEC is quite hard to understand[5]. This is because both the physical interpretations of WEC and SEC require an observer following a geodesic generated by ξ^a which is unphysical when it comes to the NEC, since it would entail an observer traveling at the speed of light (so it could follow a geodesic generated by k^a). Nevertheless,

[5] Even though both the SEC and the WEC imply the NEC.

consider a perfect fluid with Energy-momentum tensor, T_{ab} equal to

$$T_{ab} = (\rho + p)u_a u_b + p g_{ab} \tag{1.37}$$

where u_a is a unit norm timelike vector describing the fluid's four-velocity. The NEC then reads

$$\begin{aligned} & T_{ab}k^a k^b \geq 0 \\ \Leftrightarrow\ & (\rho + p)(u_a k^a)^2 \geq 0 \\ \Leftrightarrow\ & (\rho + p) \geq 0 \end{aligned} \tag{1.38}$$

which indicates that a null observer can measure the density to be negative while the pressure is positive, and vice-versa. Also, if either the density or the pressure is negative, their absolute value must be smaller than the compensating pressure or density respectively. Its necessity comes, not as an equation for matter, but as a condition on the Ricci tensor. In fact, one does not need the Einstein equations to prove the Area theorem [14].

Finally, the Area theorem states that, considering a strongly asymptotically predictable spacetime satisfying the NEC, and considering 2 Cauchy surfaces, Σ_1 and Σ_2, for the globally hyperbolic region[6] in the unphysical spacetime[7], $\tilde{V} \subset \tilde{M}$, *s.t.*, $\Sigma_2 \subset I^+(\Sigma_1)$, then the area of the Horizon at the time Σ_2, $\mathscr{H}_2 = H \cap \Sigma_2$, is greater than or equal to the area of the Horizon at the time Σ_1, $\mathscr{H}_1 = H \cap \Sigma_1$. This formulation of the theorem was taken from [4] to be consistent with the notions of asymptotical flatness and other causal structure definitions.

It is not common to find an inequality in physics. Its existence as a precise topological theorem makes it very intriguing, and in the next section, we will explore the analogy with thermodynamics which allows for the interpretation of the surface gravity as a temperature. Although this is not correct in the classical theory, Quantum Field Theory (QFT) in curved spacetime will provide a "precise"

[6] This region forcibly exists due to the strong asymptotical predictability assumption.

[7] Fictious spacetime, $(\tilde{M}, \tilde{g}_{ab})$, related to the regular spacetime by a conformal transformation, $\tilde{g}_{ab} = \Omega^2 g_{ab}$, satisfying some properties imposed by asymptotical flatness [4].

derivation of the same result in the context of Hawking Evaporation. This will be explored in section (2.2) but until then, I shall finish this section by considering the Area theorem in the context of the Kerr metric.

The area of a rotating black hole is given by

$$\begin{aligned} A &= \int_{r=r+} \sqrt{g_{\theta\theta} g_{\phi\phi}} d\theta d\phi \\ &= 4\pi \left(r_+^2 + a^2\right) \\ &= 8\pi M^2 \left(1 + \sqrt{1-\tilde{a}^2}\right) \end{aligned} \tag{1.39}$$

Differentiating this equation leads us to the result

$$\delta A = 16\pi r_+ \delta M - 8\pi M^2 \frac{\tilde{a}}{\sqrt{1-\tilde{a}^2}} \delta\tilde{a} = \frac{8\pi}{\kappa} \left(\delta M - \Omega_H \delta J\right) \geq 0 \tag{1.40}$$

which can also be written as

$$\delta M = \frac{\kappa}{8\pi} \delta A + \Omega_H \delta J \tag{1.41}$$

which shows that the properties of a rotating black hole change under a perturbation in its mass (from M to $M + \delta M$).

1.6 Black hole thermodynamics

We have now gathered all the information we need to make the analogy of black hole mechanics with thermodynamics. But first notice, as mentioned in the last section, that black hole mechanics, namely the Area theorem, are precise topological theorems whilst the thermodynamic laws are approximations; averages over a large number of microsystems. Nevertheless, there are a number of properties of black holes (I will only study the rotating case) that very much behave like thermodynamical properties, and even the number of laws in each subject seems to match. Indeed, even the idea that a thermal system will evolve into a stationary state is in accord with the idea that a black hole evolves into a stationary one [15].

Consider then the first law to be: If a stationary, axisymmetric spacetime containing a black hole of mass M and angular momentum J, with an event horizon of surface gravity κ and angular velocity Ω_H, is perturbed such that it settles down to another black hole with mass $M + \delta M$ and angular momentum $J + \delta J$, then

$$\delta M = \frac{\kappa}{8\pi}\delta A + \Omega_H \delta J \tag{1.42}$$

This is very similar to the first law of thermodynamics,

$$dU = TdS + \delta W \tag{1.43}$$

Indeed, the term $\Omega_H J$ is a work term for a rotating thermal body. The identification of the mass M with the internal energy U is also a nice analogy. It then leaves the identification of the Entropy S of the system with Area A and the surface gravity κ with the temperature T. Both interpretations answer as to what happens to the entropy of matter entering the black hole since, although the entropy of the universe decreases, which would seem to violate the second law of Thermodynamics, the area of the black hole increases. One is then led to the *generalized second law of thermodynamics* [16] considering the *generalized entropy* to be

$$S \to S + \frac{A}{4} \tag{1.44}$$

where the factor $1/4$ will be explained in section (2.2). This leaves the third law and the zeroth law. Both are relationships regarding the surface gravity, κ, as a temperature. The zeroth law tells us that when in equilibrium, the temperature is constant across the system. Similarly, the surface gravity is a constant along bifurcate Horizons [17], and it is accepted that any spacetime representing the asymptotic final state of a black hole formed by gravitational collapse may be assumed to possess a bifurcate Killing horizon [18]. However, this identification is classically impossible since a black hole is a perfect absorber and does not emit anything, hence its temperature is the absolute zero. It is not until we add QFT that this relationship can be made precise, and, as we shall see in the next chapter,

the temperature of a black hole is

$$T = \frac{\kappa}{2\pi} \tag{1.45}$$

Finally, the third law tells us that the entropy should go to zero as the temperature reaches absolute zero. The analogue would be that $\kappa \to 0$ as $A \to 0$, which, unfortunately, is not a reality. There is an alternative version of this law which states that it is impossible to achieve $T = 0$ ($\kappa = 0$) by a physical process. Although this version does seem to be correct, it is believed that the third law is not a fundamental aspect of Thermodynamics [19], and is only a summary of empirical data gathered from known substances [20]. Because of this, the fact that black holes do not obey the third law is not viewed as a failure of the analogy.

This concludes the study of black hole thermodynamics and the study of black holes in the context of General Relativity.

Chapter 2

Particle Physics in a Curved Spacetime

In this chapter I will introduce the fundamental topics of this thesis. Although they appear unrelated at first, my goal in chapter 3 and 4 will be to mix all these effects and phenomena to create a system of interesting phenomenology.

In section 1.1, I will introduce the concept of *superradiance* and primarily discuss its derivation in the context of the area theorem.

In section 1.2, I will introduce the concept of *Hawking evaporation* and focus on the basic ingredients needed to construct a QFT in curved spacetime.

In section 1.3, I will introduce the Teukolsky equation. This will facilitate the work of chapters 3 and 4 because it allows a generalization of Hawking evaporation to all spin-fields in a consistent manner.

In section 1.4, I will briefly introduce the concept of a Primordial Black Hole, motivating the initial conditions used in the following chapters in order to maximize the radiative effects of Hawking evaporation.

Finally I will briefly discuss String axions and their existence as being a consequence of having gauge theories on compact extra dimensions.

2.1 Superradiance

Superradiance (SR) is a phenomenon which is not at all restricted to black holes, but to rotating absorbing surfaces in general. In the case of a rotating black hole, it is one of the very few mechanisms one can use to extract both energy and angular momentum from the black hole. Its nature is semi-classical, meaning a quantization scheme is not necessary to predict this effect, which means that one should, and can, view this process in the context of the Area theorem presented in section 1.5. I shall present a simple derivation following the work of Beckenstein [21], and then proceed to understand it in the context of QFT.

Consider then a free massive scalar field, $\Phi = \Phi(t, r, \theta, \varphi)$, of mass μ, in the Boyer-Lindquist coordinates, which is minimally coupled to General Relativity. Its action is given by

$$S = \int d^4x\sqrt{-g}\ \left(\frac{1}{2}g^{ab}\partial_a\Phi\partial_b\Phi - \frac{1}{2}\mu^2\Phi^2\right) \tag{2.1}$$

which we can solve for the Equations Of Motion (EOM) finding the extrema using the Euler-Lagrange equations. The result is

$$\begin{aligned} &-\frac{1}{\sqrt{-g}}\partial_a\left(\sqrt{-g}g^{ab}\partial_b\Phi\right) + \mu^2 = 0 \\ \Leftrightarrow &\frac{\left(r^2+a^2\right)^2 - a^2\sin^2\theta}{\Delta\Sigma}\partial_t^2\Phi - \frac{1}{\Sigma}\partial_r\left(\Delta\partial_r\Phi\right) - \frac{1}{\Sigma\sin\theta}\partial_\theta\left(\sin\theta\partial_\theta\Phi\right) \\ &-\frac{\Delta - a^2\sin^2\theta}{\Sigma\Delta\sin^2\theta}\partial_\varphi^2\Phi + \frac{2a}{\Delta\Sigma}2Mr\partial_t\partial_\varphi\Phi + \mu^2\Phi = 0 \end{aligned} \tag{2.2}$$

We can clearly see that the only φ and t dependence on the differential equation comes in the derivatives, and one is tempted to expand Φ as

$$\Phi(t, r, \theta, \varphi) = \Phi_0(t, r)e^{-i\omega t}e^{im\varphi} \tag{2.3}$$

where ω is defined as the frequency of the wave, and m is defined as the azimuthal number. This *ansatz* exhibits the isometries of the Kerr spacetime (Stationary and Axially symmetric). This is because both ω and m are related to the Killing vectors

ξ^a and ψ^a by the Lie derivative of the field

$$\pounds_\xi \Phi = -i\omega\Phi \quad \& \quad \pounds_\psi \Phi = im\Phi \tag{2.4}$$

Consider now the action of the Killing field, χ^a, presented in section 1.3 on the scalar field.

$$\pounds_\chi \Phi = -i\left(\omega - m\Omega_H\right)\Phi(t, r, \theta, \varphi) \tag{2.5}$$

We can define a regime where the properties of the black hole affect the behavior of the field

$$\omega < m\Omega_H \tag{2.6}$$

Indeed, this regime is called the superradiant regime and can be seen to be a dynamical regime where energy and angular momentum are being extracted from the black hole directly from Hawking's Area theorem. For a wave of the form (2.3), the ratio between the angular momentum flux, $\mathcal{L}$ and energy flux, $\mathcal{E}$, at infinity is

$$\frac{\mathcal{L}}{\mathcal{E}} = \frac{m}{\omega} \tag{2.7}$$

This ratio is made trivial whenever we consider quantum mechanics, since the flux of both angular momentum and energy will just be the flux of particles times the associated quantity (ω for energy and m for angular momentum). Similarly, by conservation of energy and angular momentum, the change in energy δM and angular momentum δJ must be

$$\frac{\delta J}{\delta M} = \frac{m}{\omega} \tag{2.8}$$

Now consider the change in the area of a rotating black hole given in section 1.5

$$\begin{aligned} \delta A &= \frac{8\pi}{\kappa}\left(\delta M - \Omega_H \delta J\right) > 0 \\ \Leftrightarrow &\frac{8\pi}{\kappa\omega}\delta M\left(\omega - m\Omega_H\right) > 0 \end{aligned} \tag{2.9}$$

Considering the regime given by Eq. (2.6), in order for the area to increase, both the mass and the angular momentum of the black hole have to decrease, meaning

both quantities are being extracted from the black hole.

This brilliant argument proves that, indeed, the superradiant regime is dynamical and the black hole will evolve towards an equality in Eq. (2.6). But there are a lot of questions left unanswered. First, this is a purely classical description of the problem and one can ask if upon quantization, any subtleties arise. In fact, at the quantum level, not all possible radiation results from superradiant scattering since there is also Hawking Radiation and so, there is a mix of spontaneous superradiant scattering and Hawking Radiation [22]. Similarly, from the radial part of Eq. (2.2), which can be solved with separation of variables (see for example in [23]), we can construct a Schrödinger-like equation with a potential of the form

$$\begin{aligned} V(x) =& \big(x(x+\tau)r_+\omega + (2-\tau)(r_+\omega - m\Omega_H r_+)\big) \\ &+ x(x+\tau)\big((\tau-1)\omega^2 r_+^2 + 2(2-\tau)m\omega\Omega_H r_+^2 \\ &- r_+^2\mu^2(x+1)^2 - \lambda\big) \end{aligned} \tag{2.10}$$

where $x = \frac{r-r_+}{r_+}$, $\tau = \frac{r_+-r_-}{r_+}$ and λ is the eigenvalue of the angular part of the equation. The wave-like nature of quantum mechanics makes it so that there is a non-zero probability that the particle tunnels through the potential barrier within the potential given by Eq. (2.10) and falls into the black hole in this regime, thus violating the Area theorem [21]. Not only that but, although this proof depended heavily on the topology of the spacetime, namely the Horizon and its characteristics, the phenomenon is independent of the existence of said structure, since, as Vicente and Cardoso showed [24], it is possible to have superradiant scattering without the presence of a Horizon. Another aspect of this proof is that it fails to describe the capacity (or incapacity) of fermionic fields to experience superradiant scattering. This is because one can show that, in asymptotically flat spacetimes, the Energy-momentum tensor, T_{ab} fails to obey the WEC [25, 26], (and by analytical continuation, the NEC). Thus there is nothing we can say regarding the possibility of superradiant scattering in this proof, since the Area theorem is inapplicable to this case. Indeed, it is possible to show that fermions fail to experience superradiance [11]. This will become apparent when we consider the fermionic Gray-body

factor in section 4.2. Finally, another aspect hidden in this proof is the importance of the mass of the scalar, Φ. This is due to the form of the potential barrier which allows the trapping of low frequency modes, which results in a *superradiant instability*. A wave satisfying the superradiant condition will be trapped, reflecting back and forth with its amplitude being increased exponentially. This corresponds to having a *quasi-bound* state where we can express the frequency as

$$\omega = \omega_R + i\omega_I \tag{2.11}$$

Superradiance shall then occur when $\omega_I > 0$ and equation (2.6) shall now be an equation for the real part of the frequency. The form of each frequency can be solved analytically (see for example in [23]), under the approximation that the coupling constant is small, $\alpha_\mu = \mu M < 1$. The real part exhibits a Hydrogen-like behavior of the field

$$\omega_R = \mu\left(1 - \frac{\alpha_\mu^2}{2n^2}\right) \tag{2.12}$$

where n represents the Hydrogen-like principal quantum number, which is not surprising since the potential in Eq. (2.10) has a Coulomb-like behavior at large distances, which corresponds to the black hole's gravitational attraction. On the other hand, the imaginary part, ω_I, reflects the extremely rapid amplification of the wave

$$\begin{aligned}\omega_I = &-\frac{1}{2}\Big(\frac{l!}{(2l+1)!(2l)!}\Big)^2\frac{(l+n)!}{(n-l-1)!}\frac{4^{2l+2}}{n^{2l+4}}\times \\ &\times\prod_{k=1}^{l}\Big(k^2+16\Big(\frac{M(\omega_R-m\Omega_H)}{\tau}\Big)^2\Big)\Big(\frac{\omega_R-m\Omega_H}{\tau}\Big)\alpha_\mu^{4l+5}\Big(\frac{r_+-r_-}{r_++r_-}\Big)^{2l+1}\end{aligned} \tag{2.13}$$

where l represents the Hydrogen-like secondary quantum number, *s.t.*, $\lambda \approx l(l+1)$. From here we can see that the fastest growing state (and the only one I will be focusing on this thesis) is the analogue of the $2p$ state corresponding to the quantum numbers: $n = 2$, $l = 1$, $m = 1$, where the imaginary frequency is

$$\omega_I = -\frac{1}{12}\Big(1+16\Big(M\frac{\omega_R-\Omega_H}{\tau}\Big)^2\Big)\Big(\frac{\omega_R-\Omega_H}{\tau}\Big)\alpha_\mu^9\Big(\frac{r_+-r_-}{r_++r_-}\Big)^3 \tag{2.14}$$

After quantization, the exponentially amplified field will be interpreted as a large occupation in the superradiant states, forming a *superradiant cloud*. We will then be interested in the *eigenvalue* of the number operator, $N = \Phi^2$, as a function of time to determine the time evolution of the cloud.

$$\frac{dN}{dt} = \Gamma(M, \tilde{a}, \mu)N \tag{2.15}$$

where $\Gamma = 2\omega_I$.

Finally, from conservation of energy and angular momentum, we expect that the black hole dynamics will have a factor of the form

$$\frac{dM_{\text{sup}}}{dt} = -\mu\frac{dN}{dt} \tag{2.16}$$

$$\frac{dJ_{\text{sup}}}{dt} = -\frac{dN}{dt} \Leftrightarrow \frac{d\tilde{a}}{dt} = -\frac{dN}{dt}\frac{1}{M^2}(1 - 2\tilde{a}\alpha_\mu) \tag{2.17}$$

which is just the identification that the creation of a particle of mass μ and a quanta of angular momentum should remove a quanta of angular momentum and μ of mass from the black hole. With these last 3 equations, we can now completely describe the dynamics of both the cloud and the black hole's Degrees of Freedom (DOF).

2.2 Hawking Evaporation

Hawking radiation is one of the most important theoretical discoveries in the realm of Astrophysics because it was one of the first results calculated using a method which "combined" QFT and General Relativity (not completely, but to a reasonable degree). The idea that a black hole emits radiation was not surprising at first since one can think of superradiant scattering as a classical limit of stimulated emission. Considering also a wave propagating from $\mathscr{I}^-$ to the surface of a star collapsing, that wave would experience blueshift. If we now consider that the wave was reflected in some transient time, t_t, the reflected wave wave should travel to $\mathscr{I}^+$. But in that time, t_t, the collapsing surface would decrease, hence the blueshift effect of the incoming wave would not cancel completely the redshift of the reflected wave. Thus

we would expect particle fluxes at late times. But the idea that a black hole emits *thermal* radiation at late times was a remarkable find that allowed the Beckenstein's mathematical description of the temperature of the black hole from a mere analogy to a correct description of the thermodynamic properties of black holes.

In this section, I will pinpoint some important topics of the derivation done by Hawking in 1975 [27] utilizing the mathematical formalism used by Wald in the same year [28]. I will also focus my attention primarily on the spherically symmetric case, although a small discussion on the generalization for the Kerr case will be presented as well.

However, before discussing particle creation around black holes, first consider the consequences of quantizing a scalar field on a curved spacetime. The notion of a particle state in Minkowski spacetime is usually written with respect to some notion of time translation. This is because the Minkowski manifold admits the Poincaré group as its group of isometries, and this group contains time-translations [10]. This will also be true for stationary spacetimes, but in general one does not have a notion of time translations, hence no notion of particle states using this definition. The most usual one is to consider a suitable subspace of solutions of the classical equations [19]. As an example, let Φ denote a scalar field obeying the action defined by Eq. (2.1). By admitting that the spacetime is globally hyperbolic, one can construct a dot product on a Cauchy surface, Σ, from the natural sympletic structure of the space of solutions of the Klein-Gordon equation.

$$(\alpha \cdot \beta)_{\mathrm{KG}} = i \int_{\Sigma} (\bar{\alpha} \nabla_a \beta - \beta \nabla_a \bar{\alpha}) n^a dV \tag{2.18}$$

where α and β denote solutions of the Klein-Gordon equation, and n^a is a unit vector normal to the Cauchy surface[1]. This dot product is not positive definite, unless a convenient choice for the subspace of solutions is made. Consider then the subspace of solutions $\{f_j, j \in I\}$, with I some set of indices, s.t.,

$$\pounds_n f_j = -i\omega_j f_j \tag{2.19}$$

[1] The natural structure of the space of solutions means that the dot product is independent of the choice of the Cauchy surface [17].

where ω_j is the frequency conjugate to n^a (in the case of a stationary spacetime, we can choose $n^a = \partial_t^a$). This way we can construct the one-particle Hilbert space, $\mathscr{H}$, from the subspace $\{f_j\}$ of orthonormal solutions in Σ, with positive frequency with respect to n^a.

Consider now a spacetime which is stationary except during a certain finite time period. An example of such a spacetime is one that describes a star collapsing into a black hole. We can then define a one-particle Hilbert space before the time period in which the spacetime is non-stationary considering a scalar field solution to the Klein-Gordon equation.

$$\Phi = \sum_i \left[a_i u_i(x) + a_i^\dagger \bar{u}_i(x) \right] \tag{2.20}$$

where a_i and $a_i^\dagger$ are creation and annihilation operators obeying usual commutation relations [10]

$$[a_i, a_j] = 0 \quad \& \quad \left[a_i, a_j^\dagger \right] = \delta_{ij} \tag{2.21}$$

But the same can be made in the stationary spacetime after the non-stationary time period.

$$\Phi = \sum_i \left[a_i' u_i'(x) + (a_i')^\dagger \bar{u}_i'(x) \right] \tag{2.22}$$

where the new creation and annihilation operators also obey the usual commutation relations. The crucial part now is understanding that there is no reason for u_i' to be written as a linear combination of only positive solutions, u_i. In reality, one must expand the new modes u_i' as a linear combination of both u_i and $\bar{u}_i$.

$$u_j' = \sum_i \left(\alpha_{ji} u_i + \beta_{ji} \bar{u}_i \right) \tag{2.23}$$

where α_{ij} and β_{ij} are called *Bogoliubov coefficients*. From the othonormality of the solutions under the dot product defined by Eq. (2.18), one can uniquely determine each coefficient

$$\alpha_{ij} = (u_i' \cdot u_j) \quad \& \quad \beta_{ij} = -(u_i' \cdot \bar{u}_j) \tag{2.24}$$

which can then be used to write the new creation operators a'_i as a function of the old ones and vice-versa

$$a_i = \sum_j \left(\alpha_{ji} a'_j + \bar{\beta}_{ji} (a'_j)^\dagger\right) \tag{2.25}$$

$$a'_i = \sum_j \left(\bar{\alpha}_{ji} a_i + \bar{\beta}_{ji} a_i^\dagger\right) \tag{2.26}$$

Finally, the expectation value of each number operator for the i'th mode in the vacuum state (defined by $a'_i |0'\rangle = 0$) is

$$\langle 0'| N'_i |0'\rangle = \langle 0| (a'_i)^\dagger a'_i |0\rangle = 0 \tag{2.27}$$

$$\langle 0'| N_i |0'\rangle = \langle 0'| a_i^\dagger a_i |0'\rangle = \sum_j |\beta_{ji}|^2 \tag{2.28}$$

We can now begin the analysis of QFT in a spacetime representing spherically symmetric stellar collapse into a black hole, whose conformal diagram is depicted in Fig. 2.1. We want to study a scattering problem where the field Φ propagates from $\mathscr{I}^-$. Part of it is absorbed by the black hole but some part of the wave scatters to $\mathscr{I}^+$. The "in" and "out" one-particle Hilbert spaces are then defined as

$$\mathscr{H}_{\text{in}} = \mathscr{H}_{\mathscr{I}^-} \tag{2.29}$$

$$\mathscr{H}_{\text{out}} = \mathscr{H}_H \oplus \mathscr{H}_{\mathscr{I}^+} \tag{2.30}$$

Both $\mathscr{H}_{\mathscr{I}^-}$ and $\mathscr{H}_{\mathscr{I}^+}$ have a natural positive frequency definition, since they are flat regions in the unphysical spacetime. But $\mathscr{H}_H$ has an ambiguity in the definition of a positive frequency [28] since one could consider the frequency conjugate to both the advanced Eddigton-Finkelstein time, $v = t + r_*$, and the advanced Kruskal time, $V = T + X$ [4]. This ambiguity is avoided by computing the density matrix, ρ, since it is invariant under the choice of definition of "positive frequency". This is because a change in the time coordinate will induce a Bogoliubov transformation in $\mathscr{H}_H$. In terms of $\mathscr{H}_{\text{out}}$, this will be given by an operator which is the tensor product of the identity operator on $\mathscr{H}_{\mathscr{I}^+}$ and a unitary operator on $\mathscr{H}_H$. The density matrix is then invariant under this transformation.

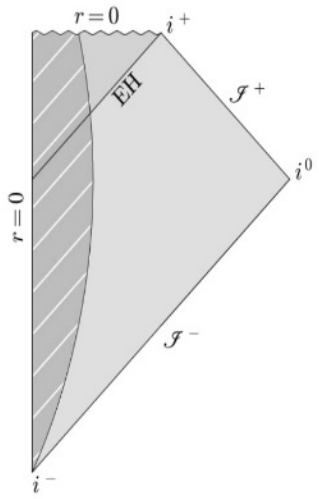

Figure 2.1: Conformal diagram representing a spherically symmetric stellar collapse into a Schwarzschild black hole. The dashed region represents the matter of the star and the rest represents a vacuum."EH" stands for event horizon.

The mathematical formalism presented by Wald was then to first consider a suitable choice for the definition of a positive frequency solution, and afterward compute the density matrix. The expected value of the number operator of the i'th mode defined on $\mathscr{H}_H$ seen from an asymptotical observer is then computed using the trace

$$\langle N_i \rangle = \mathrm{Tr}\,(N_i \rho) \tag{2.31}$$

But this was not done by Hawking in [27]. Instead, he understood that the particle density at $\mathscr{I}^+$ is also invariant under the choice of "positive frequency". But instead of calculating the particle density this way, he computed the Bogoliubov coefficients for a given time coordinate and used Eq. (2.28) to compute $\langle N_i \rangle$. His discovery was that a black hole behaves like a thermal body with temperature $T = \frac{\kappa}{2\pi}$, *i.e.*, the density of particles, per mode i, in the black hole region is

$$\langle N_i \rangle = \frac{Z_i}{e^{\frac{2\pi\omega}{\kappa}} - 1} \tag{2.32}$$

Where $Z_i = Z_i(\alpha_\mu)$ is the fraction of the wave-packet coming from $\mathscr{I}^-$ that would

have been absorbed by the black hole and is usually called the *Gray-body factor*. For the study of a collapsing body which was rotating, the same effect appears, although the frequency ω will now be replaced by $\omega - m\Omega_H$ and the Gray-body factor will now also be a function of $\tilde{a}$.

In order to understand the consequences of this effect on the black hole, one would now have to consider the back-reaction on the metric. In order to do this precisely, we would need a Quantum theory of Gravity. This is still not possible but by simple arguments of conservation of energy and momentum, it is possible to reach an approximate description of the dynamics of the black hole. In the Kerr case, if the mass (and angular momentum when allowed) decreases by the same rate at which energy is being extracted, one can then define the depletion functions f and g first introduced by Page [22]

$$\begin{pmatrix} f \\ g \end{pmatrix} = -\frac{1}{2\pi} \sum_{l,m} \int_0^\infty d\alpha_\omega \; \frac{Z_{l,m}(\alpha_\omega, \tilde{a})}{e^{\frac{2\pi(\omega - m\Omega)}{\kappa}} - 1} \Theta(\alpha_\omega - \alpha_\mu) \begin{pmatrix} \alpha_\omega \\ m/\tilde{a} \end{pmatrix} \tag{2.33}$$

where $\alpha_\omega = \omega M$ is the *dynamical coupling constant*. This way, we can describe the Hawking Evaporation (HE) of the black hole as

$$\frac{dM}{dt} = -\frac{1}{M^2} f \tag{2.34}$$

$$\frac{dJ}{dt} = -\frac{\tilde{a}}{M} g \tag{2.35}$$

We see that the mass of the black hole decreases with time and one can solve for the root of M, thus writing an expression for the lifetime of the black hole

$$\tau_{\text{lifetime}} \sim M^3 \tag{2.36}$$

We can now return to the discussion of black hole thermodynamics. The analogy between the temperature of the black hole and its surface gravity has just been made "precise". This is extremely interesting since the Area theorem did not seem to play an important role on the derivation of this result. But the topology of the horizon still plays a crucial role on this effect. Indeed it is possible to show that the

existence of this thermal term truly is a consequence of the horizon belonging to a bifurcate horizon in the extended spacetime [19]. In fact, one could suspect this idea by looking at the derivation made by Hawking [27] since there was no dependence on the details of the collapse. This is a complex concept but it connects the Hawking effect to the Unruh effect predicted a year after [29]. But one must be careful when comparing these two phenomena since, although they appear very similar, in the case of the Kerr spacetime, there is no analog of the Unruh effect [30].

2.3 Teukolsky Equation

In order to generalize the work done in the previous section, one would have to solve each individual equation for each field and calculate its Gray-body factor. In the case of spinorial fields, we would also need to change the -1 to a $+1$ in the denominator of Eq. (2.33), which is just the statement that fermions obey Fermi-Dirac statistics. Fortunately, in the case of massless fields, it has been shown by Teukolsky [31] that, not only can the equations for each field be completely separable, they can also be written as a single *master* equation. The point of this section is to introduce this master equation and briefly understand its origins.

As seen in section 1.4, the NP formalism is the adequate formalism to treat both spinorial fields and tensorial fields and it will be used in this section abundantly. Consider then the following null *vierbein* for the Kerr metric

$$l^a = \left(\frac{r^2+a^2}{\Delta}\right)\partial_t^a + \frac{a}{\Delta}\partial_\varphi^a + \partial_r^a \tag{2.37}$$

$$n^a = \left(\frac{r^a+a^2}{2\Sigma}\right)\partial_t^a + \frac{a}{2\Delta}\partial_\varphi^a - \frac{\Delta}{2\Sigma}\partial_r^a \tag{2.38}$$

$$m^a = \frac{1}{2^{\frac{1}{2}}(r+ia\cos\theta)}\left(ia\sin\theta\partial_t^a + \partial_\theta^a + \frac{i}{\sin\theta}\partial_\varphi^a\right) \tag{2.39}$$

The two former null vectors (l^a and n^a) are repeated null vectors classifying the

Kerr metric as of type D. This can also be seen from the spin-coefficients,

$$\begin{gathered}\kappa = \sigma = \lambda = \nu = \epsilon = 0 \\ \rho = -1/(r - ia\cos\theta) \quad \beta = -\bar{\rho}\cot\theta/(2\sqrt{2}) \quad \pi = ia\rho^2\sin\theta/\sqrt{2} \\ \tau = -ia\rho\bar{\rho}\sin\theta/\sqrt{2} \quad \mu = \rho^2\bar{\rho}\Delta/2 \\ \gamma = \mu + \rho\bar{\rho}(r - M)/2 \quad \alpha = \pi - \bar{\beta}\end{gathered} \tag{2.40}$$

where the fact that $\kappa = \sigma = \lambda = \nu = 0$ shows again, from the Goldberg-Sachs theorem, that the Kerr metric is of type D [11].

Now consider the electromagnetic strength tensor F_{ab}. It has 6 independent components and admits the decomposition

$$F_{ab} = 2\left[\phi_1(n_{[a}l_{b]} + m_{[a}\bar{m}_{b]}) + \phi_2 l_{[a}m_{b]} + \phi_0\bar{m}_{[a}n_{b]}\right] + \text{c.c.} \tag{2.41}$$

where the square brackets on the subscripts denotes antissymetrization, and "c.c." denote the complex conjugate of the preceding terms [31]. The components $\{\phi_0, \phi_1, \phi_2\}$ completely determine the strength tensor F_{ab} (although it has 6 independent components, the functions ϕ_i are complex). Maxwell's equations in vacuum, $\nabla_a F_{ab} = 0$, in the NP formalism are now equations relating the 3 complex components

$$(D - 2\rho)\phi_1 - (\bar{\delta} + \pi - 2\alpha)\phi_0 = 0 \tag{2.42}$$

$$(\delta - 2\tau)\phi_1 - (\Delta + \mu - 2\gamma)\phi_0 = 0 \tag{2.43}$$

$$(D - \rho + 2\epsilon)\phi_2 - (\bar{\delta} + 2\pi)\phi_1 = 0 \tag{2.44}$$

$$(\delta - \tau + 2\beta)\phi_2 - (\Delta + 2\mu)\phi_1 = 0 \tag{2.45}$$

It was then shown by Teukolsky that it is possible to get decoupled second order

separable equations for ϕ_0 and ϕ_2

$$\begin{aligned}&[(D-\epsilon+\bar{\epsilon}-2\rho-\bar{\rho})(\Delta+\mu-2\gamma)\\&-(\delta-\beta-\bar{\alpha}-2\tau+\bar{\pi})(\bar{\delta}+\pi-2\alpha)]\phi_0=0\end{aligned} \tag{2.46}$$

$$\begin{aligned}&[(\Delta+\gamma-\bar{\gamma}+2\mu+\bar{\mu})(D-\rho+2\epsilon)\\&-(\bar{\delta}+\alpha+\bar{\beta}+2\pi-\bar{\tau})(\delta-\tau+2\beta)]\phi_2=0\end{aligned} \tag{2.47}$$

After quantization, we interpret ϕ_0 as a field describing photons with right-handed chirality and ϕ_2 with left-handed chirality.

Now consider the Weyl equation in curved spacetime, $\nabla_{AA'}\Phi^A=0$. Let o^A and l^A be a dyad basis, *s.t.*, Eqs. (1.24)-(1.27) are obeyed for some $\sigma^a_{AA'}$. One possibility [11], is the trivial dyad with components

$$o^\Sigma=\begin{pmatrix}1\\0\end{pmatrix}\quad\&\quad l^\Sigma=\begin{pmatrix}0\\1\end{pmatrix} \tag{2.48}$$

forcing $\sigma^a_{AA'}$ to have the components

$$\sigma^\mu_{\Sigma\Sigma'}=\frac{1}{\sqrt{2}}\begin{pmatrix}l^\mu & m^\mu\\ \bar{m}^\mu & n^\mu\end{pmatrix} \tag{2.49}$$

The spinor Φ^A then admits the simple decomposition $\Phi^A=\chi_0 o^A+\chi_1 l^A$, which makes the Weyl equation in the NP formalism read

$$(\bar{\delta}-\alpha+\pi)\chi_0=(D-\rho+\epsilon)\chi_1 \tag{2.50}$$

$$(\Delta+\mu-\gamma)\chi_0=(\delta+\beta-\tau)\chi_1 \tag{2.51}$$

Similar to the electromagnetic tensor, it is possible to decouple these equations into 2 separable equations for each component

$$[(D+\bar{\epsilon}-\rho-\bar{\rho})(\Delta-\gamma+\mu)-(\delta-\bar{\alpha}-\tau+\bar{\pi})(\bar{\delta}-\alpha+\pi)]\chi_0=0 \tag{2.52}$$

$$[(\Delta - \bar{\gamma} + \mu + \bar{\mu})(D + \epsilon - \rho) - (\bar{\delta} + \bar{\beta} + \pi - \bar{\tau})(\delta + \beta - \tau)]\chi_1 = 0 \tag{2.53}$$

where, again, each component is a chiral component, with χ_0 having the quantum interpretation of fermions with right-handed chirality, and χ_1 with left-handed chirality.

Finally, not only is it remarkable that every physical field is decoupled and separable, they can also all be written in a single master equation. Let ψ denote a generic field. The equation

$$\begin{aligned}
&\Big[\frac{(r^2+a^2)^2}{\Delta} - a^2\sin^2\theta\Big]\partial_t^2\psi + \frac{4Mar}{\Delta}\partial_t\partial_\varphi\psi + \Big[\frac{a^2}{\Delta} - \frac{1}{\sin^2\theta}\Big]\partial_\varphi^2\psi \\
&- \Delta^{-s}\partial_r\Big(\Delta^{s+1}\partial_r\psi\Big) - \frac{1}{\sin\theta}\partial_\theta\Big(\sin\theta\partial_\theta\psi\Big) - 2s\Big[\frac{a(r-M)}{\Delta} + \frac{i\cos\theta}{\sin^2\theta}\Big]\partial_\varphi\psi \\
&- 2s\Big[\frac{M(r^2-a^2)}{\Delta} - r - ia\cos\theta\Big]\partial_t\psi + (s^2\cot^2\theta - s)\psi = 0
\end{aligned} \tag{2.54}$$

reduces to Eqs. (2.46), (2.47), (2.52), (2.53) and (2.2)[2] when the following identification is made based on the value of the *spin weight*, s

ψ	s
Φ	0
χ_0	1/2
$\rho^{-1}\chi_1$	-1/2
ϕ_0	1
$\rho^{-2}\phi_2$	-1

Table 2.1: Identification of each field for each spin s in the Teukolsky formalism

This equation also works for the spin-2 field, although I neglected to show it since we did not used it in this thesis.

At last, the separability of Eq. (2.54) can be seen through the expansion

$$\psi = e^{-i\omega t}e^{im\varphi}S(\theta)R(r) \tag{2.55}$$

[2] For the massless case: $\mu = 0$.

where $R(r)$ and $S(\theta)$ obey the equations

$$\Delta^{-s}\frac{d}{dr}\Big(\Delta^{s+1}\frac{dR}{dr}\Big)+\Big(\frac{K^2-2is(r-M)K}{\Delta}+4i\omega sr-\lambda\Big)R=0 \tag{2.56}$$

$$\begin{aligned}&\frac{1}{\sin\theta}\frac{d}{d\theta}\Big(\sin\theta\frac{dS}{d\theta}\Big)+\Big(a^2\omega^2\cos^2\theta-\frac{m^2}{\sin^2\theta}\\&-2a\omega s\cos\theta-\frac{2ms\cos\theta}{\sin^2\theta}-s^2\cot^2\theta+s+A\Big)S=0\end{aligned} \tag{2.57}$$

with $K=(r^2+a^2)\omega-am$ and $\lambda=A+a^2\omega^2-2am\omega$, and where A is a separation constant. The angular function represents a spheroidal harmonic [32], which leaves only the radial function to be solved for the Gray-body factors.

It is important to remind that the master equation is applied to a chiral component of a field, which means that, when taking into account the Standard Model, there will be a factor of 2 in the depletion function associated with the electron, muon and the tau, but not with the neutrino since neutrinos are all left-handed [33]. Similarly there will be a factor n, where n is the dimensionality of the representation of the associated symmetry group. For example the quark up transforms as a triplet under $SU(3)$, hence, there will be a factor of 12 (3 from color times 2 from chirality times 2 to consider its anti-particle) in its depletion function. I will return to this in section 4.1.

2.4 Primordial black holes

In order to maximize the radiative effects of Hawking radiation, we would like to consider black holes that are evaporating today. Such types of black holes cannot form by stellar collapse since their mass would be too high and these effects would be negligible. Instead, they can be produced by the collapse of density fluctuations in the early universe [34]. A black hole of this type is called a Primordial Black Hole (PBH)[3].

Considering that we want our black hole to evaporate today, its mass is then

[3] Although this is not the only way of producing them [35]

fixed by the time of evaporation being approximately equal to the age of the universe. Such an equation is obviously also a function of its angular momentum but the result can be approximated to $M \approx 10^{12}$ kg. These black holes have approximately the size of a proton ($r \approx 1.5$ fm).

According to the Standard Model of Cosmology [36], in order for a density fluctuation of order $\delta\rho \sim \rho$, to collapse into a black hole, the overdense region must enter the particle horizon, i.e.,

$$r = \frac{1}{H}\Big|_{\text{at formation}} \tag{2.58}$$

We can then consider the mass of the fluctuation

$$M = \frac{4}{3}\pi r^3(\rho + \delta\rho) \sim \frac{4}{3}\pi r^3\rho \sim \frac{r^3H^2}{2} \tag{2.59}$$

where one of the Friedmann equations was used [37]. We can then see from the initial consideration given by Eq. (2.58), that the mass of the overdense region is all compacted in a Schwarzschild radius, thus generating a primordial black hole.

It is widely accepted that microscopic black holes should be formed in the radiation dominated era [38] which impose some restrictions on the possible values of the initial angular momentum. From statistical analysis, it has been shown in [39, 40, 41], that the initial reduced angular momentum of PBHs should be very small. For that reason we shall consider black holes with initial conditions

$$M(t=0) = 10^{12} \text{ kg} \quad \& \quad \tilde{a}(t=0) = 0.01 \tag{2.60}$$

2.5 String Axions

The idea of an axion does not come from string theory, but from Quantum Chromodynamics (QCD). It was presented as a solution for the strong CP problem by Peccei and Quinn [42] where the CP-breaking topological Lagrangian density is

allowed by the $SU(3)$ symmetry

$$\mathcal{L} = \frac{\theta}{32\pi^2}\mathrm{Tr}\left(G_{ab}\tilde{G}^{ab}\right) \tag{2.61}$$

where G_{ab} is the gluon field strength and $\tilde{G}_{ab}$ is its dual. Although this term has no contributions in perturbation theory and does not affect the EOM (its the definition of a topological Lagrangian), it contributes, *e.g.*, to a non-zero eletric dipole moment for the neutron

$$|d_n| \approx 3.6 \times 10^{-16} e\theta \text{ cm} \tag{2.62}$$

where e is the electric charge of the electron. This result is then constrained by the experimental measurements ($\theta < 10^{-10}$) [43] which results in a fine-tuning problem where supposedly θ could take any value from 0 to 2π, yet any contribution coming from first order CP-breaking terms in the electroweak sector is cancelled by this *unrelated* gluon term.

The solution presented by Peccei and Quinn was to promote $\theta = \frac{a}{f_a}$ to a dynamical scalar field with decay constant f_a. This field has a shift symmetry generated by an anomalous $U(1)_{\mathrm{PQ}}$ symmetry, which is explicitly broken by QCD *instantons*, at a certain scale $T < \Lambda_{\mathrm{QCD}}$. This in turn, generates an effective periodic potential which relaxes the vacuum expectation value of a to zero, solving the strong CP problem while generating a mass for the axion

$$m_a = \frac{\Lambda^2_{\mathrm{QCD}}}{f_a} \tag{2.63}$$

In the case of string theory, the idea is slightly different. Axion-like fields appear from Kaluza-Klein (KK) compactifications [44, 45] as zero modes of p-forms which are fundamental in the construction of the different string theories. The underlying theory behind these axions is out of the scope of this thesis, and thus, I shall only briefly mention their properties and origins. For the purpose of this work, they can just be seen as a large number of light scalar particles which we are adding to the Standard Model.

String Theory requires a large number of dimensions (namely 10) in order to be devoid of conformal anomalies which arise by construction. These extra dimensions, in order not to be observed, are then compactified into a small scale, restoring the possible physicality of the theory. Considering the simplest case of the Neveu-Schwarz 2-form[4], B_2, the number of zero modes resulting from the compactified extra dimensions will be equal to the number of homologically non-equivalent closed two-cicles in the compactified space [46]. The complicated topology of the Calabi-Yau manifold (the compactified manifold) makes it so that the number of closed two-cicles can be very large and quickly rise through many orders of magnitude [47], resulting in a large number of string axions (tipically in the 100's-1000's) - the *axiverse*.

But these modes behave as massless scalar fields, i.e., they have a shift symmetry. The similarity with the QCD axion is now visible, since there are numerous non-perturbative effects [48, 49, 50] which can generate a periodic potential similar to the QCD axion potential, thus inducing a mass for the String Axions. There is some freedom in the masses of these axions and there should be a distribution of axions across the different orders of magnitude of their masses.

To conclude, it is important to notice that if the QCD axion is one of the string axions in the axiverse, then all axions must be light compared to the SUSY scale and the Planck scale [46]. In order to illustrate the dynamics of superradiance and Hawking evaporation, the heaviest Axion Like Particle (ALP) we will consider will have a mass of 1 GeV.

[4]Which is a fundamental field in all supersymmetric string theories.

Chapter 3

Primordial Black Hole dynamics with scalar fields

We now begin considering a universe with two particle species: A massless ALP and a 1 GeV ALP (I will also show calculations for 10 GeV and 100 MeV). The point of this exercise is to understand the dynamics of a rotating black hole undergoing evaporation of the massless ALP and Superradiance of the heavy ALP. Once we add the Standard Model plus an arbitrary number of light ALP species, we expect this scenario to be similar to a string axiverse with many light ALP species (~ 10000).

In section 3.1, we compute the Hawking Evaporation part with a massless scalar and recreate the results found by Page [22].

In section 3.2, we consider a black hole undergoing a Superradiant Instability with the 1 GeV ALP.

Afterwards, we consider both phenomenon at the same time. Since the timescale of each phenomena goes from the age of the universe to seconds, it is not surprising that there are numerical problems arising, which will be solved considering an artificial scale factor on the Superradiant timescale. The discussion of this methodology will be done in section 3.3.

Finally we conclude by showing the results and discussing the various regimes in section 3.4.

3.1 Hawking Evaporation with a light ALP

We consider the approximation that the light ALP is massless. This is motivated by the fact that we want evaporation to always be present and, considering we use a starting mass of the black hole of $M = 10^{12}$ kg, we have that $T > m$ (where m denotes the mass of the emitted particle) to be true for values smaller than ~ 10 MeV. This means that particles lighter than this mass are always being emitted and their depletion functions, $f(M, \tilde{a})$ and $g(M, \tilde{a})$, have a very small dependence on the black hole mass, and can be written as $f(\tilde{a})$ and $g(\tilde{a})$. In turn, as seen in section 2.2, the mass dependence is fixed by the dynamical coupling constant, $\alpha_\omega = \omega M$. It is then a good approximation to consider the particles as massless once the temperature of the black hole is greater than the particle's rest mass. This approximation naturally comes with consequences, and I will return to this in chapter 4, since for now, we are only considering a scalar particle. Thus, for the rest of this thesis, I will then consider masses < 10 MeV to be negligible.

As seen in the previous chapter, we need to solve the Teukolsky equation in order to find the Gray-body factors associated with massless scalar emission, so that we can calculate the depletion functions. They were calculated numerically and given to me by my colleague Marco Calzà and present the starting point of this thesis. They are a set of numerical lists characterized by $(l, m, \tilde{a})$, and written as a function of α_ω in accordance with [22, 51, 52]. This data was also used by Calzà, Rosa and March-Russell [1] and so we expect that our results will be similar to them. Considering a mode (l, m) and a fixed $\tilde{a}$, this data was a set of 600 points starting from $\alpha_\omega = 0.004$, and ending at $\alpha_\omega = 2.4$. In order to calculate (f, g), we integrate the Gray-body factors and sum over all modes.

$$\begin{pmatrix} f \\ g \end{pmatrix} = -\frac{1}{2\pi} \sum_{l,m} \int_0^\infty d\alpha_\omega \, \frac{Z_{l,m}(\alpha_\omega, \tilde{a})}{e^{\frac{2\pi(\omega - m\Omega)}{\kappa}} - 1} \begin{pmatrix} \alpha_\omega \\ m/\tilde{a} \end{pmatrix} \tag{3.1}$$

The integration method used was the simple rectangle rule and the approximation $0.004 \approx 0$ and $2.4 \approx \infty$ was used. I will now proceed to motivate this approximation. The Phase Space, $\mathcal{S}$, of this system will consist of the dynamical properties of

the black hole $(M, \tilde{a})$ as well as the number of heavy ALPs, N, produced via Superradiance, together with their time derivatives. As seen in section 2.4, a black hole which is evaporating today and was formed in early universe, has an initial mass of $\sim 10^{12}$ kg. Also, because of numerical resolution, our computations will only evolve until $\sim 10^6$ kg (which is fine because a black hole of this mass takes less than a second to evaporate). This means that the subset, $\mathcal{P}$, of physical solutions is constrained by $M \in [10^6\ , 10^{12}]$ kg. For a given frequency, ω, of the light ALP, this will impose a range for the integrand. Written in SI units, we have

$$\alpha_\omega \simeq 2.4 \left(\frac{M}{10^6 \text{ kg}}\right)\left(\frac{\omega}{0.66 \times 10^6 \text{ GeV}}\right) \tag{3.2}$$

$$\alpha_\omega \simeq 0.004 \left(\frac{M}{10^{12} \text{ kg}}\right)\left(\frac{\omega}{1.1 \text{ MeV}}\right) \tag{3.3}$$

for the lowest lower bound and the highest upper bound for the frequency. This then shows that we are integrating across 9 orders of magnitude when running through the values of $M \in \mathcal{P}$, starting at $\omega \sim 1$ MeV. This, in turn, is ≈ 0 according to the initial approximation made in this section, thus showing that the approximation is consistent and valid. For a fixed (l, m) mode, we also have a list of 7 points, from $\tilde{a} = 0.01$ to $\tilde{a} = 0.6$. I will now motivate why the data only reaches $\tilde{a} = 0.6$. As seen in section 2.4, we are considering black holes with very low initial angular momentum ($\tilde{a}[t = 0] = 0.01$). As proven in [22, 52], the maximum reduced angular momentum the black hole can achieve is the asymptotic value of $\tilde{a} = 0.555$. This can be seen by looking at the depletion function that governs the reduced angular momentum $h(\tilde{a})$

$$\frac{d\tilde{a}}{dt} = -\frac{\tilde{a} f(\tilde{a}) h(\tilde{a})}{M^3} \tag{3.4}$$

where $h(\tilde{a}) = -\frac{g(\tilde{a})}{f(\tilde{a})} + 2$. This function has a root which means that there is a value of $\tilde{a}$, *s.t*, its time derivative is null. But in the case of scalar emission, the reduced angular momentum must always change during Hawking emission (for the l=0 mode: although $J = aM$ is the same, M decreases, thus increasing $\tilde{a}$). This then proves that the black hole will evolve towards the root of $h(\tilde{a})$, hence showing why it is only necessary to study until $\tilde{a} = 0.6$, since until the black hole reaches

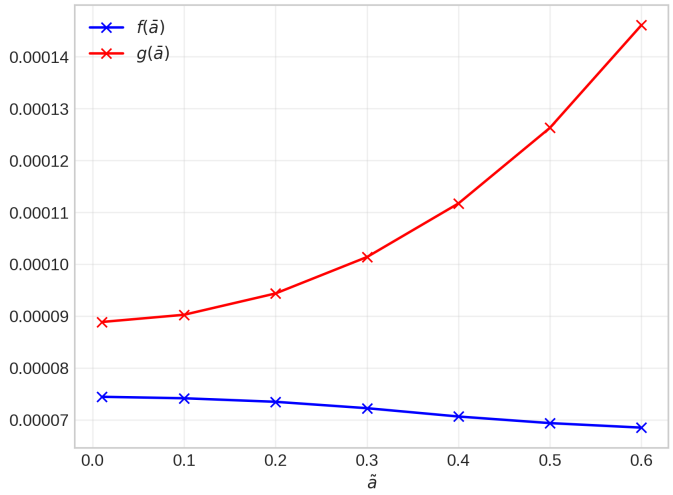

Figure 3.1: Depletion functions, (f, g), of a massless scalar field as a function of the reduced angular momentum, $\tilde{a}$.

the asymptotic value of 0.555, it never surpasses it.

In order to generate more data, a fit of a polynomial function of order 6 was made. This means that we have 5 extrema and 4 inflection points. The motivation for this choice is that it is equivalent to the one made in [1]. The results for the interpolation were

$$\begin{aligned} f(\tilde{a}) =& 0.0000744174 + 2.25708 \times 10^{-6}\tilde{a} - 0.0000865978\tilde{a}^2 + 0.000562244\tilde{a}^3 \\ & - 0.00219359\tilde{a}^4 + 0.00379048\tilde{a}^5 - 0.00231514\tilde{a}^6 \end{aligned} \tag{3.5}$$

$$\begin{aligned} g(\tilde{a}) =& 0.0000900149 - 0.0000797337\tilde{a} + 0.00125308\tilde{a}^2 \\ & - 0.00578823\tilde{a}^3 + 0.0135512\tilde{a}^4 - 0.0144944\tilde{a}^5 + 0.00589463\tilde{a}^6 \end{aligned} \tag{3.6}$$

Although an interpolation of $h(\tilde{a})$ was possible, it was chosen to be kept as $h(\tilde{a}) = -\frac{g(\tilde{a})}{f(\tilde{a})} + 2$.

The EOM governing the dynamics of a black hole radiating a single massless

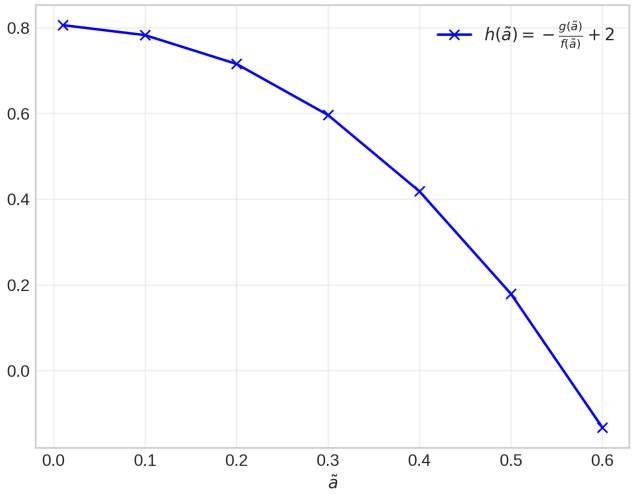

Figure 3.2: Depletion function, $h(\tilde{a})$, of a massless scalar field as a function of the reduced angular momentum, $\tilde{a}$. The root of this function represents the asymptotic value of the reduced angular momentum of the black hole on the last stages of evaporation.

scalar field are

$$\begin{cases} \frac{dM}{dt} = -\frac{f(\tilde{a})}{M^2} \\ \frac{d\tilde{a}}{dt} = \frac{\tilde{a}}{M^3}\left(-g(\tilde{a}) + 2f(\tilde{a})\right) \end{cases} \tag{3.7}$$

These equations present a set of stiff differential equations to be solved numerically. The methods used by both Python and Wolfram Mathematica were "Radau" and "BDF". Both presented very similar results, although the "BDF" method was able to converge approximately twice as fast. The resulting "Regge" plot is shown in Fig. 3.3.

As seen in section 2.1, superradiance is an effect which extracts both angular momentum and mass from the black hole, which means that it will always be pulling the curve in Fig. 3.3 downwards. Similarly, since fermions and other higher spin fields cannot emit in the $l = 0$ mode, they will also always extract angular momentum and mass from the Black Hole. It is then clear that this result represents the upper bound on the black hole reduced angular momentum of this type of plot.

For Fig. 3.4 and Fig 3.5, the chosen list of times, t, was a set of 1000 equidistant

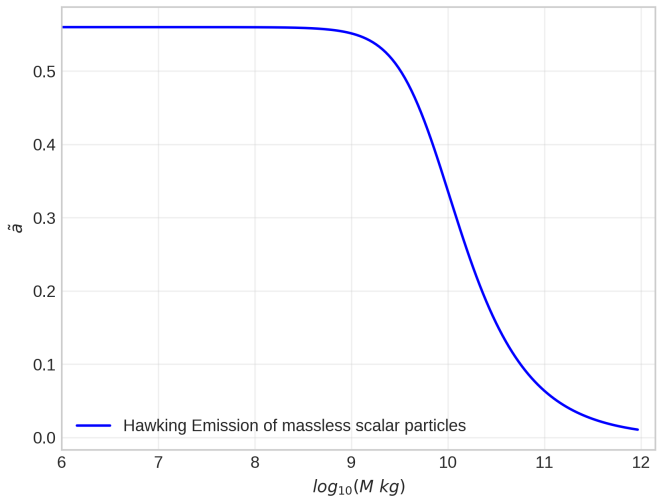

Figure 3.3: "Regge" plot of Hawking emission of a massless scalar field by a black hole with initial with initial conditions given by Eq. (2.60). Its asymptotic value of $\tilde{a}$ can be seen to be $\tilde{a} \sim 0.555$, which denotes the maximum value of reduced angular momentum possible in all of the scenarios studied in this thesis.

points on a logarithmic scale from its creation to its complete evaporation. But it is clear that most of the dynamics only occurs in the final moments of the black hole. This an important aspect since the "Regge" plots might be misleading in the sense that, although the graph represents all of the possible configurations of the PBH in this universe, for most of its life, the PBH will be in the first point (or very close to it) which is just the initial conditions.

3.2 Superradiance with a scalar

We now focus our attention on the study of a superradiant instability with a massive scalar, in continuation with the study made in the previous section. A black hole with very low initial angular momentum ($\tilde{a}_0 = 0.01$) will rotate faster and faster as time passes due to Hawking scalar emission. It is then possible to achieve a configuration in which a superradiant instability is triggered and a large number of heavy ALPs is produced. But the dynamical DOF of the PBH are not the

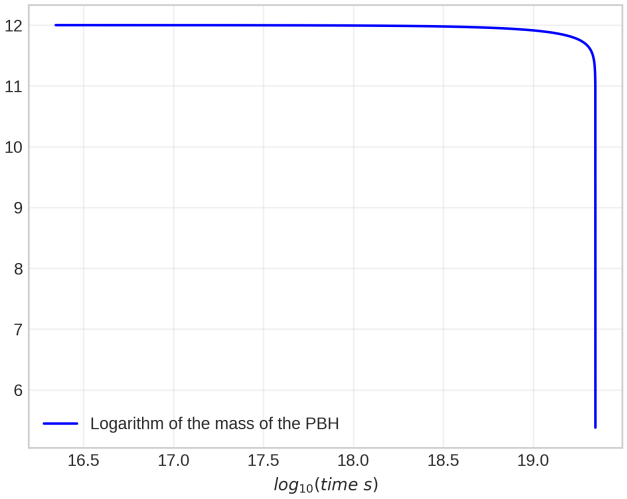

Figure 3.4: Mass of the PBH as a function of time for pure scalar emission via Hawking Radiation of a massless scalar in a PBH with initial conditions given by Eq. (2.60). It is visible that a black hole of this mass formed in the early universe will not have evaporated today and still retains most of its mass. This is because it is only emitting a massless scalar field instead of the whole Standard Model.

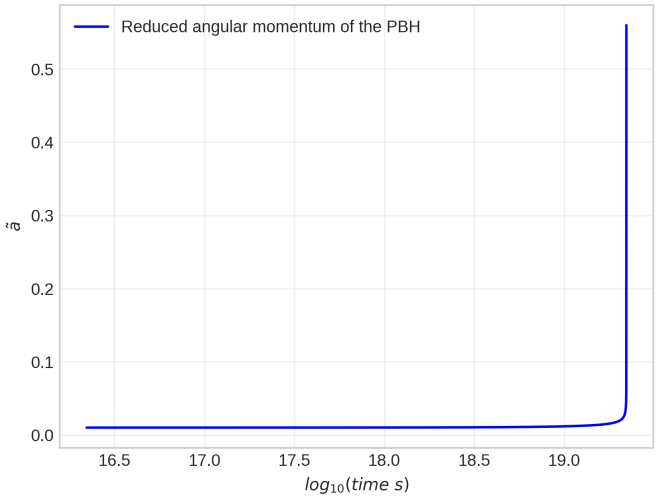

Figure 3.5: Reduced angular momentum of the PBH as a function of time for pure scalar emission via Hawking Radiation of a massless scalar in a PBH with initial conditions given by Eq. (2.60).

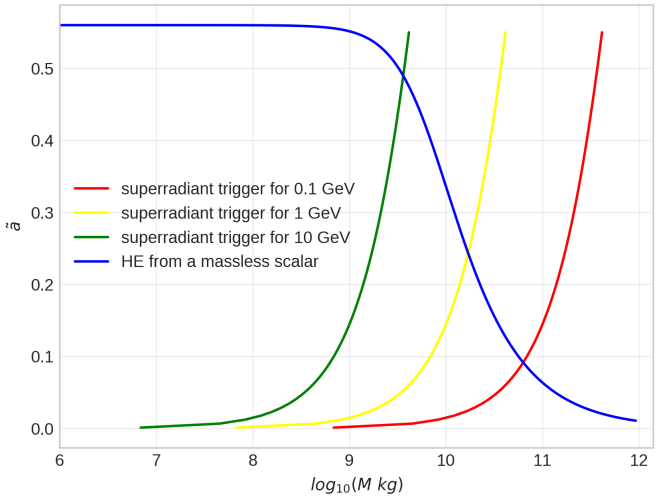

Figure 3.6: Superradiant trigger for various masses of the heavy ALP (100 MeV, 1 GeV, 10 GeV) superposed on Fig. 3.3

only functions related to the instability. Indeed, the mass plays a huge role in defining when the instability is triggered, which can be seen in Eq. (2.6). Let $\mathcal{R} = \left[10^6 \text{ kg}, 10^{12} \text{ kg}\right] \times (0, 0.555]$ denote the subspace of canonical variables in phase space $(M, \tilde{a})$ in the purely evaporating system[1]. One can compute the contour lines of the superradiant trigger equation for different masses of the heavy ALP in $\mathcal{R}$, and intersect them with the evaporation "Regge" trajectory as seen in Fig. 3.6. I will now motivate the choice of the mass of the heavy ALP. For masses orders of magnitude below 1 GeV, superradiance would be negligible due to the α_μ^9 term in the superradiant rate. Similarly, for masses orders of magnitude above 1 GeV, we start deviating from the initial phenomenology discussed in section 2.5, since the many ALPs in the axiverse cannot be very heavy in order to contain the QCD axion. Hence we are left with the three values in Fig. 3.6. We chose a mass of 1 GeV because we still want to give time for $\tilde{a}$ to increase, but also cannot allow it to be very high since then there would not be an intersection between the trajectory and the superradiant threshold, once we add the Standard Model and the large

[1] This is the "Regge" plot region in Fig. 3.3.

number of light ALP species. I will return to this in the next chapter.

Focusing our attention on the mass of the heavy ALP of 1 GeV, the intersection point of the "Regge" trajectory with the superradiant trigger is the upper bound on the possible values of $\tilde{a}$ allowed on a small region of $\mathcal{R}$ (there is a possibility that after superradiance becomes negligible, the Hawking evaporation brings the trajectory upwards to the asymptotic value of $\tilde{a} = 0.555$).

For a heavy ALP of 1 GeV and a black hole with an initial mass of 10^{12} kg, the maximum coupling constant is $\alpha_\mu \approx 0.04$ when the trigger happens. This means that we can use the expression in Eq. (2.14) for the imaginary part of the frequency (half of the superradiant rate). Similarly, the intersection is made at approximately $\tilde{a} = 0.224$ which means that we can approximate the expression for the superradiant rate of the dominant mode for low values of $\tilde{a}$ approximating the outer horizon to the Schwarzschild radius and the inner radius to the Schwarzschild's singularity, and approximating the frequency to the mass of the heavy ALP, leaving us with the simple expression:

$$\Gamma = \frac{1}{24} \left(\tilde{a} - 4\alpha_\mu\right) \alpha_\mu^8 \mu \tag{3.8}$$

For this range of masses we now have to create a consistent methodology to solve the EOM for the system. This is because Eqs. (2.16) and (2.17) are only valid whenever Eq (2.6) is obeyed. This is actually not true since, for energy values greater than $m\Omega_H$, the decay rate, Γ, is negative, which is just the statement that particles are being absorbed by the black hole. But in order to solve these equations, we need initial conditions for the number of heavy ALPs at the point of the trigger. This is because if we were to consider a quantum fluctuation ($N = 1$) at the formation of the PBH, we would not have a physically interesting instability since the particle would just be absorbed much earlier than the superradiant instability. One could imagine multiplying the superradiant rate by a step function in the frequency, $\Gamma \to \Gamma\Theta(\omega - m\Omega_H)$. But this does not account for a potential reabsorption of the cloud after formation. This is a possible scenario once we add fermions because Hawking evaporation can decrease $\tilde{a}$ and make $\Gamma < 0$ after the cloud forms. In order to solve this, let t_s denote the first instance, numerically speaking, *s.t.*,

$\tilde{a} \geq 4\alpha_\mu$ (this is just the superradiant trigger equation with the approximations defined above), with M and $\tilde{a}$ starting from the initial conditions defined in section 2.5 and evolving with the HE Eqs. (3.7). It has the physical interpretation of the time where a quantum fluctuation occurs in the superradiant regime. Now we can multiply the superradiant rate by a step function but this time in the time

$$\Gamma \to \Gamma\Theta(t - t_s) \tag{3.9}$$

After the time, t_s, the superradiant term will always exist which means that potential reabsorption can happen. The system of equations is now a little bit more complicated but can be written in a concise form

$$\frac{dM}{dt} = -\frac{f(\tilde{a})}{M^2} - \mu\Gamma N\Theta(t - t_s) \tag{3.10}$$

$$\frac{d\tilde{a}}{dt} = \frac{\tilde{a}}{M^3}(-g(\tilde{a}) + 2f(\tilde{a})) - \frac{\Gamma\Theta(t - t_s)N}{M^2} \tag{3.11}$$

$$\frac{dN}{dt} = \Gamma\Theta(t - t_s)N \tag{3.12}$$

with initial conditions

$$M(t = 0) = 10^{12}\ \text{kg} \quad \tilde{a}(t = 0) = 0.01 \quad N(t = t_s) = 1 \tag{3.13}$$

where the approximation $(1 - 2\tilde{a}\alpha_\mu) \approx 1$ was made in Eq. (3.11).

3.3 Hawking Evaporation plus Superradiance

The analytical developments made in the previous section, although simple in theory, are extremely hard to solve in practice. This is because of the difference in values that the rates for superradiance and Hawking evaporation take. To make this precise let $f : \mathbb{R}^+ \to \mathbb{R}^+$ denote a $C^{>0}$ function with coordinates x. We can define the *timescale*, τ_f, of the function f with respect to x as

$$\frac{1}{\tau_f} = \left|\frac{1}{f}\frac{df}{dx}\right| \tag{3.14}$$

We can use this function to calculate the "size" of the derivative and compare each phenomenon. To each dynamical DOF of the black hole, there will be 2 timescales associated with Hawking evaporation and superradiance respectively, while for the number of heavy ALPs we will only have the timescale associated with superradiance.

$$\tau_M^{\rm HE} = \frac{M^3}{f(\tilde{a})} \quad \tau_{\tilde{a}}^{\rm HE} = \frac{M^3}{|-g(\tilde{a}) + 2f(\tilde{a})|} \tag{3.15}$$

$$\tau_M^{\rm SR} = \frac{M^2}{\alpha_\mu \Gamma N} \quad \tau_{\tilde{a}}^{\rm SR} = \frac{\tilde{a}M^2}{\Gamma N} \quad \tau_N = \frac{1}{\Gamma} \tag{3.16}$$

Both intra and inter phenomena timescale relations are interesting. First consider the intra timescale relations for each phenomena. The ratio between the reduced angular momentum and the mass timescales is just a ratio of depletion functions for Hawking evaporation, namely $1/|f(\tilde{a})h(\tilde{a})| = 1/|-g(\tilde{a}) + 2f(\tilde{a})|$ and $1/f(\tilde{a})$, which is just $|1/h(\tilde{a})|$. This is a ratio of order 1 at lower values of $\tilde{a}$ but quickly diverges at the late stages of evaporation. This has the nice interpretation that the initial conditions do not really matter for the final value of $\tilde{a}$, since it will always evolve to the asymptotic value. This will be very important since superradiance will dominate early and decrease the values of $\tilde{a}$, but once superradiance stops being important (once the mass is sufficiently low, *s.t.*, $\Gamma N \approx 0$), Hawking evaporation will dominate and still take $\tilde{a}$ to the asymptotic value.

In the case of superradiance, the ratio between the reduced angular momentum and the mass timescales is just the coupling constant times the reduced angular momentum, $\alpha_\mu \tilde{a}$, which is much smaller than one[2]. Indeed the order of magnitude at the trigger is 10^{-4} which is the highest possible value in the subset of $\mathcal{R}$ below the Hawking evaporation scalar trajectory. This ratio tells us of the importance of the coupling constant in the timescale of superradiance, which decreases by 6 orders as the mass follows the "Regge" trajectory in $\mathcal{R}$.

Finally, consider inter phenomenon timescale relations. The two ratios between

[2] This was seen in Eq. (3.11) when the approximation $1 - 2\alpha_\mu \tilde{a} \approx 1$ was made.

the same DOF are

$$\frac{\tau_M^{\rm HE}}{\tau_M^{\rm SR}} = \frac{\alpha_\mu M\Gamma N}{f(\tilde{a})} \tag{3.17}$$

$$\frac{\tau_{\tilde{a}}^{\rm HE}}{\tau_{\tilde{a}}^{\rm SR}} = \frac{M\Gamma N}{|-g(\tilde{a})+2f(\tilde{a})|\tilde{a}} \tag{3.18}$$

These results are not as trivial as the previous ones. One reason for this is that we can no longer compute these ratios as trajectories in $\mathcal{R}$. This is because the new phase space also contains N as a canonical variable (together with its time derivative). Fortunately, N is bounded by the properties of the black hole as follows: A particle created by the black hole due to superradiance will take a quanta of angular momentum. Then for the primary mode the number of particles created is directly related to the total angular momentum extracted, *i.e.*, $\Delta N = \Delta J$. One can then find an approximate expression for the total number of heavy ALPs created considering that the change in the mass of the PBH is $\delta M \approx 0$

$$\begin{aligned} \delta\tilde{a} = \frac{\delta J}{M^2} &= \frac{\delta N}{M^2} \\ \Leftrightarrow \Delta N &= M^2\Delta\tilde{a} \end{aligned} \tag{3.19}$$

We can then consider an approximate form of the upper bound for N, having a change in the reduced angular momentum equal to the total reduced angular momentum of the PBH the instant the superradiance is triggered

$$N_{\rm max} = M^2\tilde{a} \tag{3.20}$$

This means that the sub-region of canonical variables in the new phase space is then $\mathcal{R}' \approx \mathcal{R} \times [1, M^2\tilde{a}]$, with $(M, \tilde{a}) \in \mathcal{R}$. This then allows for the computation of the different timescales. However, it is worth understanding the possible solutions in $\mathcal{R}'$ a little bit more before jumping to numerical data. In Eqs. (3.16), the timescale of N, $\tau_N = \Gamma^{-1}$, comes multiplied by N in the equations for the dynamical properties of the black hole. We also know that superradiance should be much stronger than HE. But we know that the values of $(M, \tilde{a})$ before the trigger must come by the evolution given by Eqs. (3.7), *i.e.*, only through HE. We can then ask if Γ itself is

enough to win HE, *i.e.*, if the ratio given by Eq. (3.18) is equal to 1 with $N = 1$ and sensible values of $(M, \tilde{a})$.

$$\begin{aligned} \tau^{\rm HE}_{\tilde{a}} &= \tau^{\rm SR}_{\tilde{a}} \\ \Leftrightarrow \tilde{a} &= \frac{4\alpha_\mu}{1 - \frac{24}{\alpha_\mu^9}\frac{|-g(\tilde{a})+2f(\tilde{a})|}{N}} \equiv \frac{4\alpha_\mu}{1-\epsilon} \end{aligned} \tag{3.21}$$

We would then expect ϵ to be small ($\ll 1$) in order to expand $\tilde{a} = 4\alpha_\mu(1+\epsilon)$, which is just the statement that superradiance starts dominating close to the superradiant threshold. But from Figs. 3.1 and 3.2, we know that $|-g(\tilde{a}) + 2f(\tilde{a})| \sim 10^{-5}$, and we also know that $\alpha_\mu \sim 10^{-3}$, which means that $\epsilon \sim 10^{23}/N = 10^{23}$, if $N = 1$, thus proving, by *reductio ad absurdum* that Γ, by itself, is not a sufficient indicator of the timescale of superradiance with respect to the dynamical properties of the black hole and is not large enough to dominate over HE by itself, since, if $N = 1$, $\epsilon > 1 \Rightarrow \tilde{a} < 4\alpha_\mu$, which is a contradiction since the superradiant regime imposes that $\tilde{a} > 4\alpha_\mu$. But Γ is still an indicator of the timescale of N, which means it serves to have an idea of the time it takes to form the cloud and is then still important since numerically, the equations are solved for the same time.

When comparing the timescale of M due to HE and the timescale of N, one immediately finds a problem. Looking at Fig. 3.7 we see that, for large values of the mass, around $M \sim 10^{10}$ kg, if we choose units, *s.t.*, Γ has numerical precision, we will not have numerical resolution for the HE part in the differential equations. Similarly, in the same values of M, if we choose units, *s.t.*, $f(\tilde{a})/M^2$ has numerical precision, we will not have numerical precision for the superradiant part of the equations[3]. This constitutes a timescale problem that must be solved in order to have convincing results. One could consider a non linear transformation on the coordinates loosing the physical interpretation of the DOF of the system in order to always have numerical precision and resolution throughout the calculation. This type of transformations usually come with the cost of increasing the time of convergence of the code since more operations have to be made. Instead, we chose to multiply Γ by an artificial constant scale factor, $10^{-\xi}$, with $\xi \geq 0$, to "slow

[3] The same happens to the angular part, but the discrepancy is not as large.

down" and ensure precision and resolution in the early stages in the computation. The physical case occurs when $\xi = 0$ and the purely evaporating system occurs when $\xi = \infty$. This comes with the cost that at the late stages of evolution, the superradiant factor will go to zero much earlier (numerically speaking), but by computing the same system of equations for various values of ξ, we were able to approximately extrapolate the correct results for the evolution of both the cloud and the black hole.

We then expect the correct trajectory through $\mathcal{R}$ as follows: from the initial conditions until the point $(M(t_s), \tilde{a}(t_s))$, the trajectory should follow exactly the one from pure scalar Hawking emission. Afterwards the instability will occur and a large number of heavy ALPs will be produced almost discontinuously from the point of view of $\mathcal{R}$. Then, an equilibrium state should occur where the trajectory should lie on top of the orbit defined by Eq. (3.21) with $N \approx N_{\max}$, *i.e.*, on top of the superradiant trigger orbit. Finally, close to $M \sim 10^7$ kg, the superradiant rate should decay immensely due to the α_μ^8 factor, and HE should dominate the system bringing the trajectory back to the asymptotic value of $\tilde{a} = 0.555$.

The minimum value of $\tilde{a}$ should be highly dependent on ξ, since ξ can be interpreted as a vertical shift upwards of the timescale of N. The lower the value of ξ, the higher the intersection point between the timescales and the lower the value of M associated with the minimum of $\tilde{a}$. This means that, in the physical case, it takes a long time for HE to start dominating and spin up the black hole.

3.4 Results

We consider a time $t_s : M(t_s) = 10^{10.208}$ kg and $\tilde{a}(t_s) = 0.252$ and study ξ values going from 15 to 7. The reason for only studying until $\xi = 7$ was that the time it takes for the codes to run would increase tremendously and even stop converging for values $\xi < 7$. We also now consider a time translation, *s.t.*, $t \to t - t_s$. This is just the statement that, since we already know the dynamics for $t < t_s$, the numerical calculations only started at t_s. This also means that the results will run until we reach the time that a black hole of mass $M = 10^{10.208}$ kg takes to evaporate, which

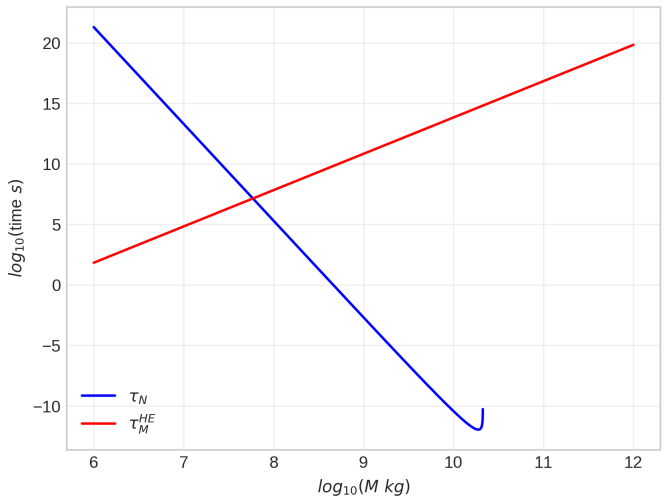

Figure 3.7: Value of the timescales of the HE part of the mass of the black hole as well as the timescales of the number of heavy ALPs in an orbit defined by $\tilde{a} = 0.3$ as a function of the mass of the PBH.

is $\sim 10^{14}$ s. The allowed values of ξ depend heavily on the mass of the heavy ALP chosen. The higher the mass, the lower the possible value of ξ that still had numerical precision. But even though we only go so far in decreasing ξ, we can still understand very well the results by looking first at the constants under changes in ξ. From Figs. 3.8 and 3.9, we see that only the initial regime seems to depend on ξ. This is because ξ only affects directly the timescale of N, *i.e*, the time it takes to form the initial cloud, while the timescale of the dynamical properties of the black hole depends on ΓN. This means that once the cloud is formed, even though Γ is now weaker, the number of heavy ALPs allows superradiance to still be the dominant phenomenon and allows the stabilization of the trajectory back to the orbit of superradiant threshold, hence showing why only the initial regime depends visually on ξ.

Lastly, by looking again at Figs. 3.8 and 3.9, there is a pseudo-equilibrium behavior very similar to March-Russell and Rosa's work in [53]. After the large number of heavy ALPs are created in the cloud, we get an equilibrium condition

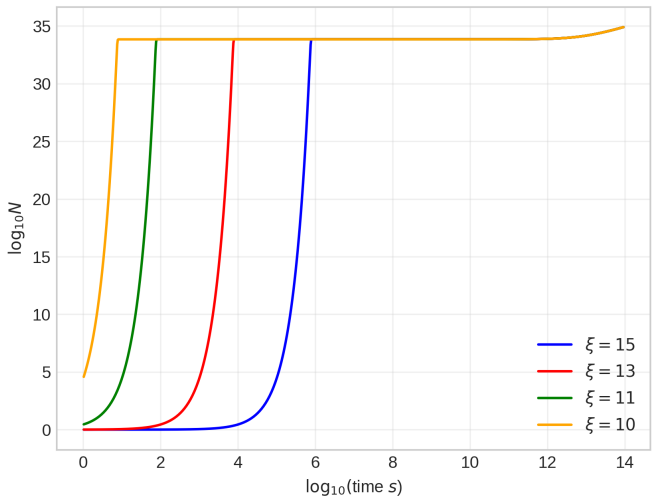

Figure 3.8: Number of 1 GeV ALPs in the superradiant cloud for various values of ξ as a function of time in the system defined on Fig 3.10.

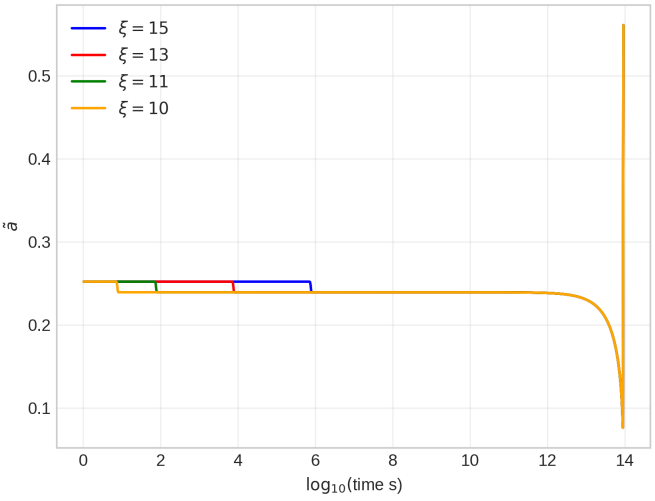

Figure 3.9: Reduced angular momentum of the PBH for various values of ξ as a function of time in the system defined on Fig 3.10.

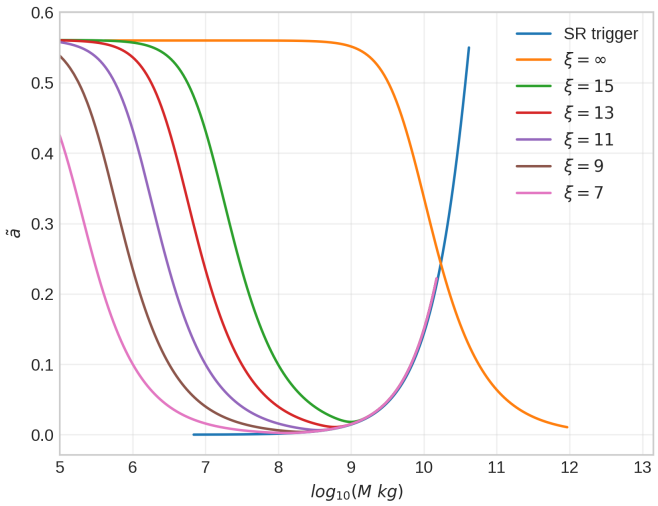

Figure 3.10: "Regge" trajectories for various values of ξ for a black hole whose evolution is given by Eqs. (3.10), (3.11) and (3.12) with initial conditions given by Eq. (3.13). The minimum value of $\tilde{a}$ for the different ξ is shifting to lower masses just like how the intersection point in the timescales in Fig. 3.7 moves as ξ changes. The case $\xi = \infty$ is just the result from Fig. 3.3.

from Eq. (3.11)

$$\Gamma = \frac{4\mu(-g(\tilde{a}) + 2f(\tilde{a}))}{N} \tag{3.22}$$

that is achieved once the superradiance condition (Eq. (2.6)) is nearly saturated. But, contrary to [53], where HE spins down the PBH and makes $\Gamma < 0$, *s.t*, the cloud reabsorption maintains the PBH spin, here HE spins up the PBH, and therefore $\Gamma > 0$, which maintains the PBH spin by producing more heavy ALPs. This is, of course, temporary since the equilibrium equation (Eq. (3.22)) also informs us that there is still a non-zero rate of ALPs being created in the cloud, which can be seen in both Figures. At $\approx 10^{13}$ s, the number of ALPs starts increasing significantly and the equilibrium can no longer be sustained. As the number of ALPs in the cloud increases in these late times, the reduced angular momentum decreases. This behavior is seen in Fig. 3.10 with support from Fig. 3.11 as the subsection of the trajectory which lies on the superradiant trigger orbit. Finally, the

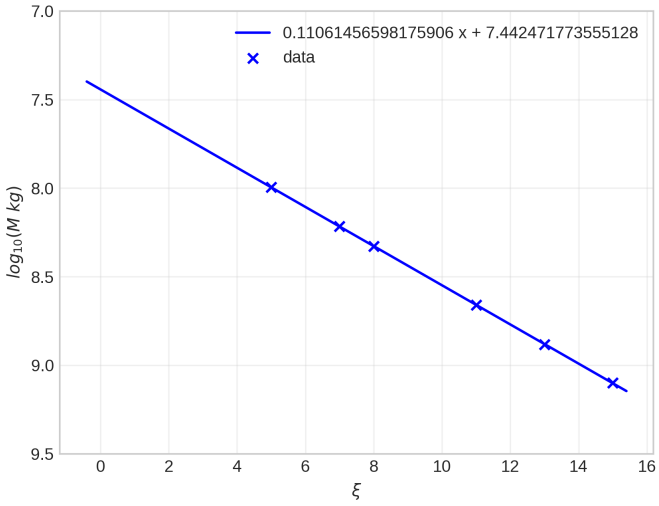

Figure 3.11: Extrapolation of the minimum of M, *s.t.*, $\tilde{a} = 4\alpha_\mu$ in the system defined on Fig 3.10. We see that in the physical case (ξ=0), the minimum would occur at $M \approx 10^{7.44}$ kg which is consistent with the region in Fig. 3.7 after the intersection where HE starts dominating.

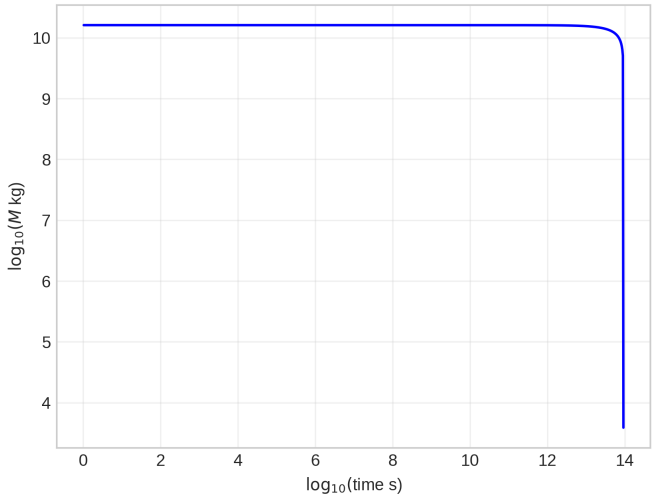

Figure 3.12: Mass of the PBH for $\xi = 15$ as a function of time in the system defined on Fig 3.10. Contrary to the other DOF of the system, the PBH mass is barely affected by superradiance, thus why we only show the result for one ξ. It would be the same for any ξ.

mass starts depleting due to HE as seen in Fig. 3.12, which nullifies the importance of superradiance due to the factor α_μ^8 in the superradiant rate, and we are left with a purely evaporating system, and thus, the reduced angular momentum starts increasing until it reaches the asymptotic value of $\tilde{a} = 0.555$.

This concludes the study of this toy model and we are ready to include the Standard Model particles as well as the axiverse. We expect the behavior to be similar for large values of the number of light ALP species in the axiverse emitted by HE.

Chapter 4

Primordial Black Hole dynamics in the String Axiverse

We now begin the final chapter of this thesis where we consider a more physical model compared to the one introduced in the previous chapter by adding the Standard Model of Particle Physics as well as an arbitrary number of light ALP species (with masses lower than 10 MeV).

In the first section, I will introduce the particles considered and how to incorporate them in the system of equations. Although the starting point was the Gray-body factors from the Teukolsky equation, which are valid for massless particles, one can still infuse some information about the mass of the particle in the depletion function. This methodology will be discussed in section 4.1.

Afterwards we will immediately see an inconsistency when taking into account the QCD degrees of freedom. Due to the approximations made, we will be forced to consider a non-trivial choice which will involve prioritizing the $\Lambda_{\rm QCD}$ phase transition instead of the Black-body behavior of the black hole. This discussion will be made in section 4.2.

Finally, we present the results with the new DOF exploring the various regimes created by considering different numbers of light ALP species in our axiverse in section 4.3.

4.1 Standard Model

Similarly to how we started the previous chapter, we begin by considering that all the particles in the our theory are massless. This was motivated in section 3.1, but the main idea is that we consider an axiverse of primarily light ALP species with mass < 10 MeV, where we considered ≈ 0 as the initial approximation to make sure the black hole is always emitting the light ALPs through Hawking radiation. We also considered the particles in the Standard Model as massless so we can use the Gray-body factors that were already calculated by my colleague Marco Calzà by solving the Teukolsky equation. But the consideration that the black hole is evaporating all of the Standard Model at all times is extremely flawed since one can still incorporate information about the mass of the particle in its depletion functions. For a massive particle of spin s, the depletion functions take the form

$$\begin{pmatrix} f_s \\ g_s \end{pmatrix} = -\frac{1}{2\pi} \sum_{l,m} \int_0^\infty d\alpha_\omega \; \frac{Z^s_{l,m}(\alpha_\omega, \tilde{a})}{e^{\frac{2\pi(\omega - m\Omega)}{\kappa}} - (-1)^{2s}} \Theta(\alpha_\omega - \alpha_\mu) \begin{pmatrix} \alpha_\omega \\ m/\tilde{a} \end{pmatrix} \tag{4.1}$$

We can still use Eq. (4.1) simply by replacing the Gray-body factor $Z^s_{l,m}(\alpha_\omega, \tilde{a})$ by a massless one. Then, for an orbit of $\tilde{a}$ (without loss of generality, it was chosen $\tilde{a} = 0.3$ in Figs. 4.3 and 4.4), we can integrate numerically resulting in a function of the coupling constant α_μ. By choosing a specific particle (again, without loss of generality, the charm quark was chosen in the same figures) to have the depletion functions written as functions of the mass of the PBH, which has a one-to-one correspondence to its temperature, in a given orbit of $\tilde{a}$. What we then see is that the temperature dependence of the depletion functions behaves very much like a logistic type of function except it is not centred around the mass of the particle but instead, there is a *Wien displacement* of ≈ 5 as seen in Figs (4.3) and (4.4), which can be approximated by a step function. This displacement is, of course, consistent

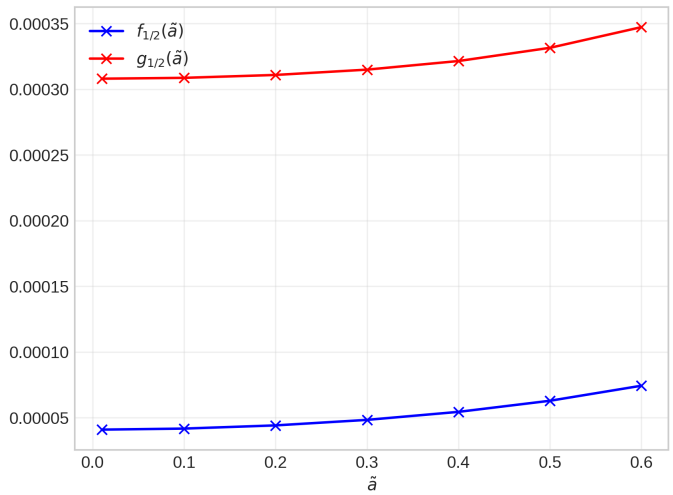

Figure 4.1: Depletion functions, (f, g), of a massless spinor field as a function of the reduced angular momentum, $\tilde{a}$.

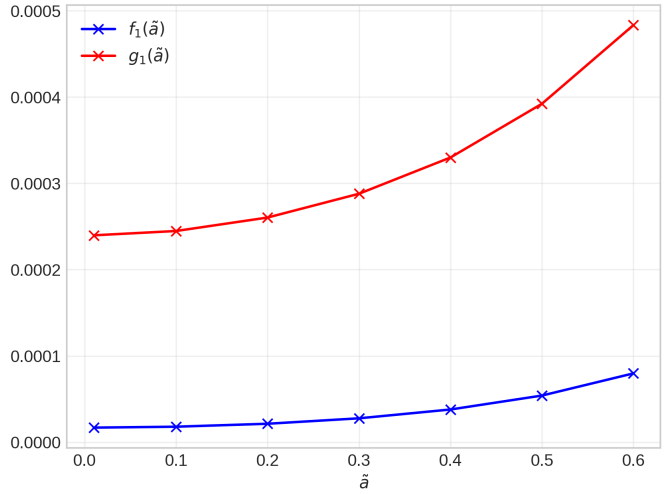

Figure 4.2: Depletion functions, (f, g), of a spin 1 field as a function of the reduced angular momentum, $\tilde{a}$.

with the idea that the black hole is a black-body, but will create a problem once we consider the QCD degrees of freedom later.

With a consistent methodology to incorporate massive particles, we can now integrate the angular part of the depletion functions and extrapolate in order to have more data for the numerical integration. Again, a polynomial fit of order 6 was chosen for consistency reasons:

$$f_{1/2}(\tilde{a}) = 0.0000430872 - 0.000147724\tilde{a} + 0.00210828\tilde{a}^2 - 0.0103186\tilde{a}^3 + 0.0237358\tilde{a}^4 - 0.0250602\tilde{a}^5 + 0.00995142\tilde{a}^6 \tag{4.2}$$

$$g_{1/2}(\tilde{a}) = 0.000312487 - 0.00030137\tilde{a} + 0.00421135\tilde{a}^2 - 0.0210962\tilde{a}^3 + 0.0486298\tilde{a}^4 - 0.051424\tilde{a}^5 + 0.0205077\tilde{a}^6 \tag{4.3}$$

$$f_1(\tilde{a}) = 0.0000284354 - 0.000791532\tilde{a} + 0.0109718\tilde{a}^2 - 0.0552645\tilde{a}^3 + 0.127075\tilde{a}^4 - 0.134093\tilde{a}^5 + 0.05321\tilde{a}^6 \tag{4.4}$$

$$g_1(\tilde{a}) = 0.000263771 - 0.00164255\tilde{a} + 0.0230689\tilde{a}^2 - 0.114924\tilde{a}^3 + 0.264679\tilde{a}^4 - 0.279658\tilde{a}^5 + 0.111251\tilde{a}^6 \tag{4.5}$$

Finally all that is left is to enumerate the Standard Model degrees of freedom and their masses. The QCD DOF still need a bit more discussion but for now consider the following DOF of the Standard Model plus the axiverse minus QCD in Table 4.1. We also did not consider the graviton since its effect was negligible for HE [22].

Very briefly, we have 2 polarizations for each lepton, except the neutrinos since they are all left-handed. There are also 2 polarizations for the photon and the Weak gauge bosons Z, W^+ and W^-. Finally there are 4 Higgs DOF since the Higgs field is a complex field which is a natural representation of $SU(2)$ ($2 \times 2 = 4$). The

Name	Mass	DOF
ALPs	$m_a = 0$	n_a
Photons	$m_\gamma = 0$	2
Neutrinos	$m_\nu = 0$	6
Electron	$m_e = 0$	4
Muon	$m_\mu = 105.7$ MeV	4
Tau	$m_\tau = 1.776$ GeV	4
Z boson	$m_Z = 91.2$ GeV	2
W boson	$m_W = 80.4$ GeV	4
Higgs boson	$m_H = 125$ GeV	4

Table 4.1: DOF of each type of particle together with their respective masses according to the initial approximation of section 3.1 (not counting the QCD DOF)

number of light ALP species in the axiverse is a variable but the numbers studied were 0, 100, 200, 400, 500 and 1000 also for consistency reasons (these numbers were also studied in [1]). There is also a factor of 2 in each particle that has an anti-particle.

4.2 Quantum Chromodynamics degrees of freedom

The problem with QCD in our theory is that there is a phase transition at $\Lambda_{\rm QCD} \approx 250$ MeV, and below this temperature there are no free quarks [33]. This obviously comes with a problem, since, if we incorporate quarks in our theory, they would be observed below $\Lambda_{\rm QCD}$ since, *e.g.*, the mass of the up quark is ≈ 2.16 MeV [54]. The solution presented by MacGibbon and Webber [55] is to consider new effective masses for the QCD particles as seen is Table 4.2. The main idea of these effective masses is to divide the mass of the proton into the 3 quarks (up and down), but there is still a problem. By considering the depletion functions given by Eq (4.1), due to the *Wien displacement*, there would still be a non-zero flux of up and down quarks below $\Lambda_{\rm QCD}$. This occurs because we solved the Teukolsky equation which is an equation for free particles, and the phase transition is just a condition we imposed *a posteriori*. In order to solve this, one would have to solve the QCD Lagrangian in curved spacetime which is still impossible. We decided to follow the

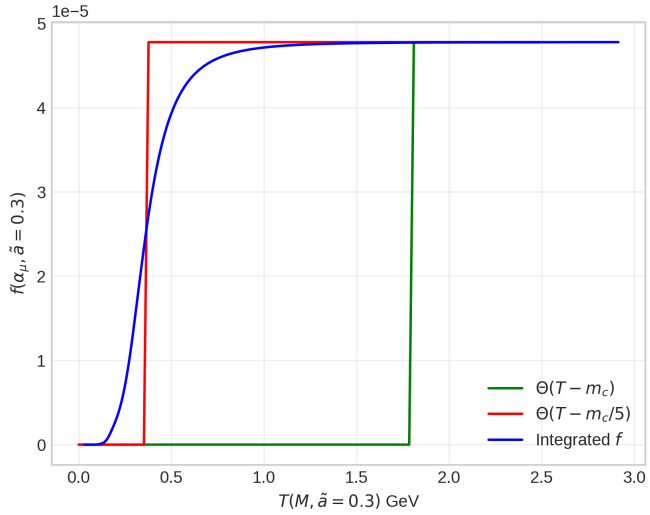

Figure 4.3: Temperature dependence of the mass depletion function of the black hole for the charm quark in an orbit of $\tilde{a} = 0.3$, with two step functions identifying the inflection point of $f(\alpha_\mu, \tilde{a} = 0.3)$ and the mass of the charm quark.

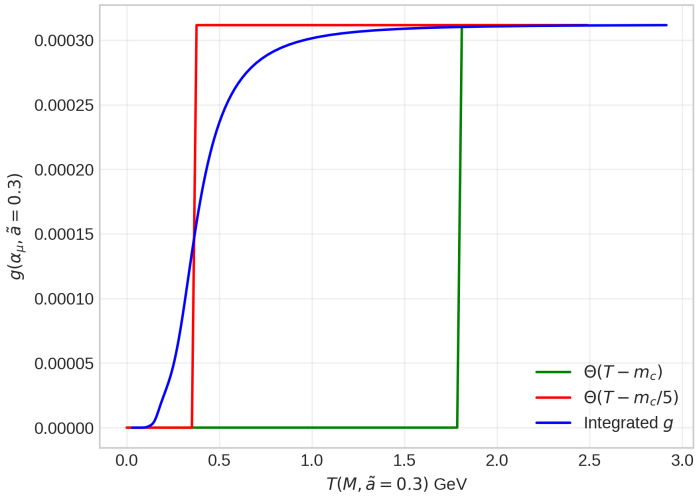

Figure 4.4: Temperature dependence of the angular momentum depletion function of the black hole for the charm quark in an orbit of $\tilde{a} = 0.3$, with two step functions identifying the inflection point of $f(\alpha_\mu, \tilde{a} = 0.3)$ and the mass of the charm quark.

Name	Mass	DOF
Up	$m_u = 0.320$ GeV	12
Down	$m_d = 0.320$ GeV	12
Strange	$m_s = 0.500$ GeV	12
Charm	$m_c = 1.80$ GeV	12
Bottom	$m_b = 5.20$ GeV	12
Top	$m_t = 50$ GeV	12
Gluon	$m_g = 0.600$ GeV	16

Table 4.2: Number of DOF of each type of particle together with their respective effective masses from [55].

standard procedure in the literature [55] of considering the mass dependence of the depletion functions as a step function on the effective mass of the particle. This is the statement of instead considering Eq. (4.1), we considered the equation

$$\begin{pmatrix} f_s \\ g_s \end{pmatrix} = -\frac{1}{2\pi} \sum_{l,m} \Theta(T-m) \int_0^\infty d\alpha_\omega \, \frac{Z^s_{l,m}(\alpha_\omega, \tilde{a})}{e^{\frac{2\pi(\omega - m\Omega)}{\kappa}} - (-1)^{2s}} \begin{pmatrix} \alpha_\omega \\ m/\tilde{a} \end{pmatrix} \tag{4.6}$$

which means that we are prioritizing the QCD phase transition more than the black body behavior of the black hole.

Below $\Lambda_{\rm QCD}$, although we do not have emission of free quarks, we can still emit hadrons. The particles with a mass below $\Lambda_{\rm QCD}$ are the pion mesons (π^0, $\pi^\pm$) which we considered to be emitted in the range $T \in [m_\pi, \Lambda_{\rm QCD}]$.

Finally we updated some of the masses to agree with [54]. The complete set of DOF is shown in Table (4.3) and in order to incorporate all of these DOF into the depletion functions, we considered a linear combination similar to Page [22]

$$\begin{aligned} f(\tilde{a}) = &\Big(n_a + 3(\Theta(T-m_\pi) - \Theta(T-m_{\Lambda_{\rm QCD}})) + 4\Theta(T-m_H)\Big) f_0(\tilde{a}) \\ &+ \Big(6 + 4\Theta(T-m_e) + 4\Theta(T-m_\mu) + 4\Theta(T-m_\tau) + 12\Theta(T-m_u) + 12\Theta(T-m_d) \\ &+ 12\Theta(T-m_s) + 12\Theta(T-m_c) + 12\Theta(T-m_b) + 12\Theta(T-m_t)\Big) f_{1/2}(\tilde{a}) \\ &+ \Big(2 + 16\Theta(T-m_g) + 2\Theta(T-m_Z) + 4\Theta(T-m_W)\Big) f_1(\tilde{a}) \end{aligned} \tag{4.7}$$

and the same for $g(\tilde{a})$ replacing f by g.

Name	Mass	DOF
ALPs	$m_a = 0$	n_a
Photons	$m_\gamma = 0$	2
Neutrinos	$m_\nu = 0$	6
Electron	$m_e = 0$	4
Muon	$m_\mu = 105.7$ MeV	4
Tau	$m_\tau = 1.776$ GeV	4
Z boson	$m_Z = 91.2$ GeV	2
W boson	$m_W = 80.4$ GeV	4
Higgs boson	$m_H = 125$ GeV	4
Up	$m_u = 0.320$ GeV	12
Down	$m_d = 0.320$ GeV	12
Strange	$m_s = 0.500$ GeV	12
Charm	$m_c = 1.80$ GeV	12
Bottom	$m_b = 5.20$ GeV	12
Top	$m_t = 173$ GeV	12
Pion	$m_\pi = 0.139$ GeV	3
Gluon	$m_g = 0.600$ GeV	16

Table 4.3: Number of DOF of each type of particle together with their respective masses according to the initial approximation of section 3.1 and according to [55].

4.3 Results

Similarly to how we did in the previous chapter, we begin by considering just HE to understand the correct initial conditions for the final system. Looking at Fig. 4.5, we see that the edges of the graph match perfectly the points where the black hole starts emitting a certain particle. Then by looking at Fig. 4.6, we can see that the intersection of the "Regge" trajectory with the superradiant threshold orbit changes depending on the number of light ALP species. We also see that for both 0 and 100 there is no intersection. This means that we can focus only on the cases of $n_a = 200$, $n_a = 400$, $n_a = 500$ and $n_a = 1000$. For these values, we considered

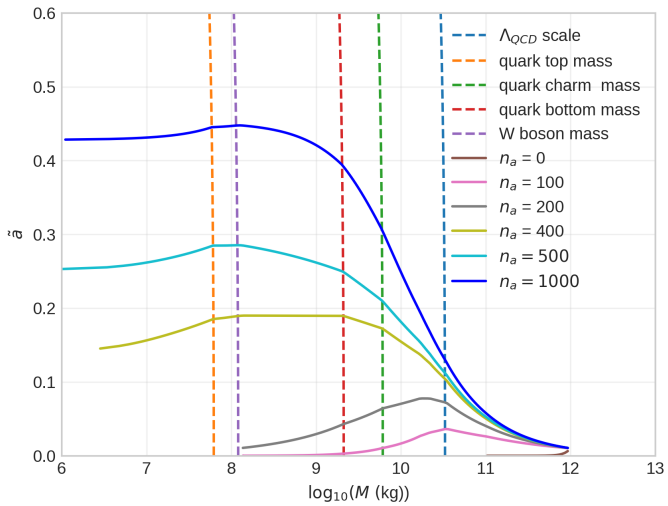

Figure 4.5: "Regge" trajectories for various numbers of light ALP species in the axiverse with only HE, in a PBH with initial conditions given by Eq. (2.60). There are also various orbits of T for the heavier particles (quark top, bottom, charm and W boson) to identify the edge points in the graph as the roots of the step functions in the depletion functions.

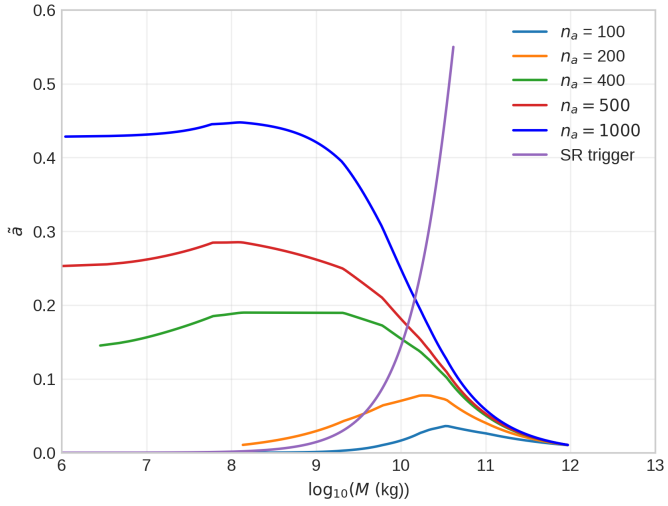

Figure 4.6: "Regge" trajectories for various numbers of light ALP species, in the system defined in Fig. 4.5, together with the superradiant trigger orbit for 1 GeV in order to understand the initial conditions for each number of light ALP species.

the initial conditions

$$n_a = 200: \quad M(t_s) = 10^{9.54}\ \text{kg} \quad \& \quad \tilde{a}(t_s) = 0.053 \tag{4.8}$$

$$n_a = 400: \quad M(t_s) = 10^{10}\ \text{kg} \quad \& \quad \tilde{a}(t_s) = 0.155 \tag{4.9}$$

$$n_a = 500: \quad M(t_s) = 10^{10,04}\ \text{kg} \quad \& \quad \tilde{a}(t_s) = 0.177 \tag{4.10}$$

$$n_a = 1000: \quad M(t_s) = 10^{10,13}\ \text{kg} \quad \& \quad \tilde{a}(t_s) = 0.216 \tag{4.11}$$

These points were chosen as the closest points numerically possible to the superradiant threshold. Again, since we already know the trajectory up until t_s, we considered a time translation $t \to t - t_s$. But this time, since the value of initial conditions depends on the number of light ALP species in the axiverse, the number of heavy ALPs in the cloud should change, as seen in Eq. (3.19). For the same change in $\tilde{a}$ (which is around ≈ 0.01), the ratio of the number of particles in the cloud after saturation of the superradiant condition for an axiverse of 200 light ALP species and 400 light ALP species is

$$\frac{N_{200}}{N_{400}} \approx \left(10^{0.5}\right)^2 = 10 \tag{4.12}$$

which means we expect 10 times more heavy ALPs in the cloud after the initial instability. Similarly, due to the α_μ^8 factor in the superradiant rate, we also expect a very large difference in the time of formation of the cloud

$$\frac{\Gamma_{200}}{\Gamma_{400}} \approx \left(10^{0.5}\right)^8 = 10000 \tag{4.13}$$

thus predicting that the time needed to form the initial cloud is ≈ 10000 times larger for the axiverse with 200 light ALP species.

Finally, before understanding the numerical results, it is also important to notice that although an axiverse of 100 light ALP species does not suffer the superradiant instability for a heavy ALP of mass $\mu = 1$ GeV, it does suffer it for a heavy ALP of $\mu = 100$ MeV. This idea of lowering the mass of the heavy ALP is worth discussing since, as shown in [1], and as seen in our replica of the calculation in Fig

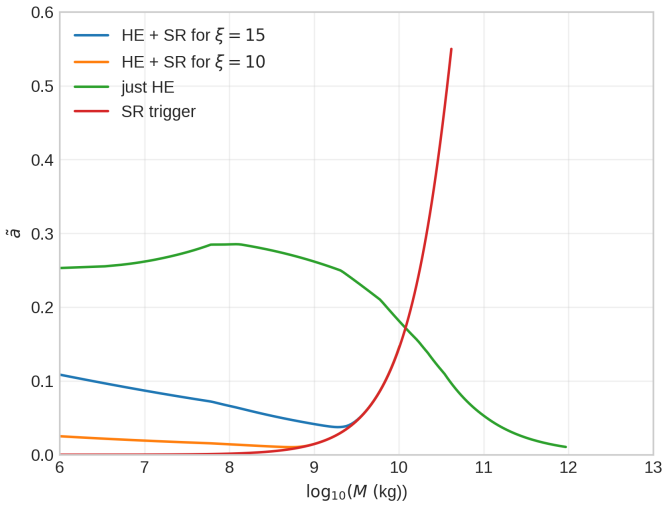

Figure 4.7: "Regge" trajectories for 2 values of ξ in an axiverse with 500 light ALP species for a black hole, whose evolution is given by Eqs. (3.10), (3.11) and (3.12) with initial conditions given by Eq. (3.13) and $f(\tilde{a})$ and $g(\tilde{a})$ defined by Eq. (4.7).

4.5, for an axiverse of 100 light ALP species, the angular momentum asymptotes to 0 as the black hole evaporates. This means that there is the possibility of *reabsorption of the cloud* since it is a similar scenario to the one shown by in [53], though only with a lot of fine tuning could reabsorption be observed. This is because by lowering the mass of the particle, the intersection occurs while the HE rate is still positive, which means there is no reabsorption. Lowering the number of light ALP species even more would then force lowering the mass of the heavy ALP to ensure the intersection, but would also still happen earlier while the HE is positive again. Only for extremely specific values of n_a and μ can one observe reabsorption, and so, it shall remain as an open subject for future work. Consider now Figs. 4.7, 4.8 and 4.9. The behavior of the trajectories is very similar to the one predicted in the previous sections and the toy model used in the previous chapter, as seen in Fig. 3.10. We see now that for values of $n_a < 500$, the asymptotic value seems now very close to $\tilde{a} = 0$ as ξ decreases. This in an extremely interesting result because our artificial *scale factor* is now drastically changing the behaviour of the trajectory,

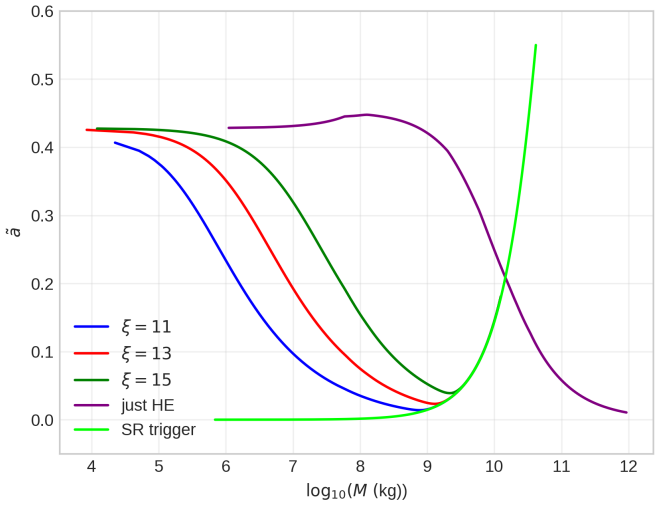

Figure 4.8: "Regge" trajectories for various values of ξ in an axiverse with 1000 light ALP species, in the system defined on Fig. 4.7.

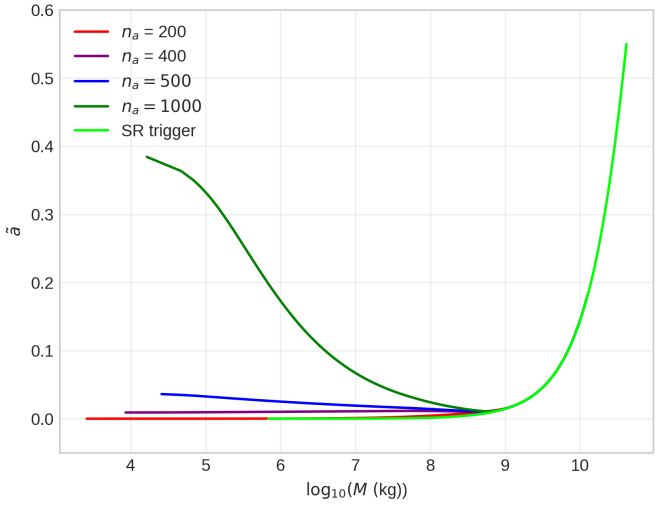

Figure 4.9: "Regge" trajectories for various numbers of light ALP species in the axiverse for $\xi = 10$, in the system defined on Fig. 4.7.

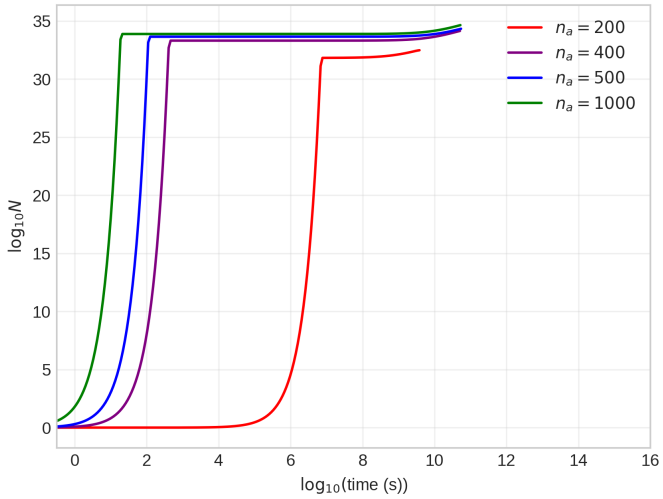

Figure 4.10: Number of 1 GeV ALPs in the superradiant cloud for $\xi = 10$, for various numbers of light ALP species in the axiverse as a function of time, in the system defined on Fig. 4.7.

instead of just shifting it, as it did in the toy model in the previous chapter. For larger values of n_a, as seen in Fig 4.8, the behavior is very similar to the one seen in the previous chapter. But for lower values of n_a, the trajectory through $\mathcal{R}$ is just the superradiant threshold orbit, the properties of the black hole at the late stages of evaporation stop being an astrophysical signature of the axiverse. Nevertheless, looking at the number of particles in the superradiant cloud at the late stages (Fig. 4.10), there is a one-to-one correspondence with $N(t = \text{today})$ and n_a, since $N(t = \text{today})$ is $\approx$ the maximum number of particles allowed by superradiance (Eq. (3.20)), which is a function of the data of the Black-Hole at the trigger which is unequivocally determined by n_a, for values of $n_a > 150$ to allow the intersection between the purely evaporating trajectory with the superradiant trigger orbit.

Finally, considering Fig. 4.12, it is clear that, for values of $n_a < 500$, we no longer have the final growth of the reduced angular momentum. This is the biggest difference between this physical model and the toy model used in the previous chapter. Both the number of particles in the cloud and the mass of the black hole depicted in Figs. 4.10 and 4.11, respectively, shows an extremely similar behavior

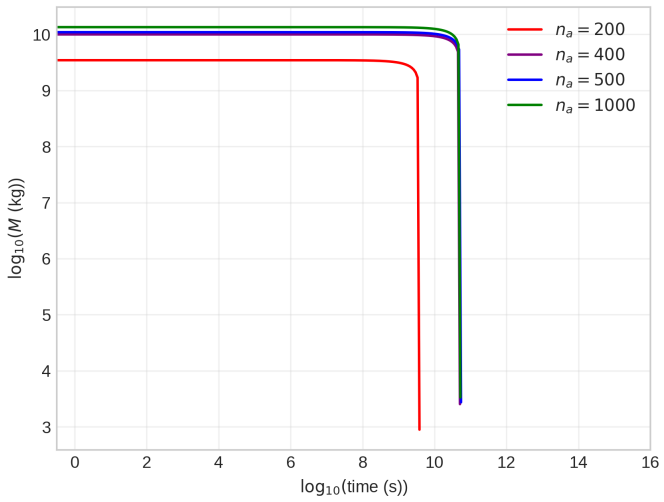

Figure 4.11: Mass of the PBH for $\xi = 10$, for various numbers of light ALP species in the axiverse as a function of time for the late stages, in the system defined on Fig. 4.7.

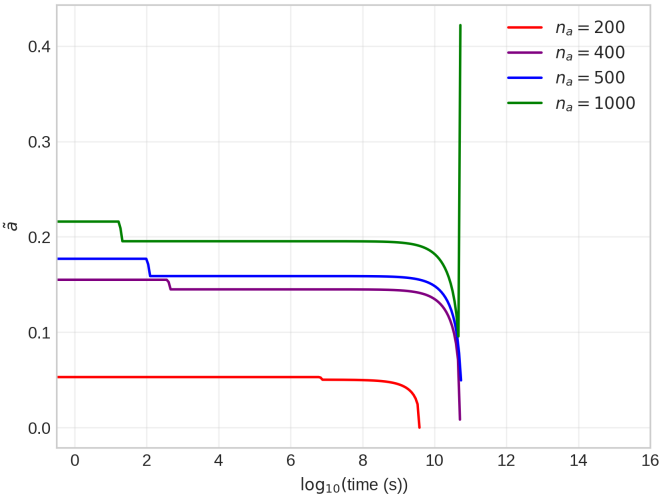

Figure 4.12: Reduced angular momentum of the PBH for $\xi = 10$, for various numbers of light ALP species in the axiverse as a function of time, in the system defined on Fig. 4.7.

to the toy model. This is because the mass is still approximately constant with respect to superradiance, and the number of particles depends more on the trigger conditions of the black hole than on the trajectory itself. Thus we are left with a very predictable result with interesting physical consequences.

Chapter 5

Conclusions

I shall begin this chapter with a recap of the results shown in chapter 4. A black hole which is formed by a density fluctuation in the early universe with an initial mass of 10^{12} kg and reduced angular momentum of 0.01 will start evaporating, increasing its reduced angular momentum due to the high number of light ALP species. For a number of light ALP species $\gtrsim 150$, the black hole will evolve in such a way that it will trigger a superradiant instability of a 1 GeV heavy ALP. The number of heavy ALP's in the superradiant cloud will depend heavily on the number of light ALP species since the intersection point with the superradiant threshold will occur at different masses for the black hole[1]. After the formation of the cloud, the black hole's dynamics will be fixed by the superradiant threshold, similar to an attractor, where Hawking evaporation will tend to increase the reduced angular momentum as the mass of the black hole decreases, whilst superradiance will always evolve towards the equality in the fundamental relation, $\omega < m\Omega_H$. This equilibrium will last until the mass gets low enough that superradiance cannot compete anymore with Hawking evaporation, and the reduced angular momentum increases very rapidly until it asymptotes to a value which is a function of the number of light ALP species in the axiverse.

[1] Notice the angular momentum will also be different but the mass influences the maximum number much more drastically than the reduced angular momentum as seen in Eq. (3.20).

From the point of view of the cloud, once a quantum fluctuation occurs in the superradiant regime, a large number of heavy ALP's will be produced in a time-span dictated by the superradiant rate, Γ. That number of heavy ALP's in the cloud depends on the properties of the black hole, *i.e*, it is a function of the number of light ALP species. After the initial growth of the cloud, a pseudo-equilibrium regime will stabilize the number of particles populating it, relating the superradiant rate and the HE rate as seen in Eq. (3.22). The non-zero superradiant rate will afterward generate more heavy ALP's approximating the number in the cloud to the maximum allowed by the black hole, until the black hole evaporates, once the instability is triggered.

One can now ask what happens to the cloud once the black hole evaporates. In this thesis, we did not consider the axion-photon coupling. To lowest order, this coupling usually comes via a fermionic loop which can be approximated to a vertex of the form [46]

$$\mathcal{L} = \frac{C\alpha_{\rm EM}}{4\pi f_a} a \epsilon^{abcd} F_{ab} F_{cd} \tag{5.1}$$

where C is a constant of order ~ 1 in $SU(5)$ GUT's, and $\alpha_{\rm EM}$ is the fine structure constant. The decay rate is then

$$\Gamma_{\rm decay} \approx \frac{\alpha_{\rm EM}^2}{256\pi^3} \frac{\mu^3}{f_a^2} \tag{5.2}$$

This is of course model-dependent since the factor f_a may vary on different string theories. But we can think backwards and consider what the appropriate f_a values are, *s.t.*, the mean-life of the heavy ALP is equal to the time it takes the black hole to evaporate, once the instability occurs. We find that $f_a \sim 10^{14}$ GeV which is close to the GUT scale, thus in agreement with string theory [46]. The actual expression for this f_a is very complicated since it depends on the time of evaporation of the black hole once the instability triggers, which has a non-trivial dependence on the number of light ALP species, since they dictate the intersection between the purely evaporating trajectory with the superradiant threshold. The photon flux due to the decay is important and, for future work, shall be added to the Hawking radiation

photon flux already calculated by Rosa, Calzà and March-Russell [1].

We also did not consider self-interactions between the heavy ALP's in the cloud. This effect has been studied by Baryakhtar, Galanis, Lasenby and Simon [56] and the idea is to "draw" Feynman-like diagrams where the "in" and "out" states are either different superradiant modes or states representing a free state and a "doomed" state, *i.e*, a state representing a particle which falls down the black hole. The mathematical description of these diagrams is given by the addition of higher order terms in N, coupled to superradiant rates of various modes in the differential equations. The consequence of the addition of these interactions is that now there is an $N_{\rm eq}$, *s.t.*, $\frac{dN}{dt} = 0$. This means that we will have an equilibrium and if $N_{\rm eq} < N_{\rm max}$, then these effects should have an important contribution to the dynamics. Due to the complexity in the implementation of the dynamics, it was left for future work, although we expect self interactions to play a negligible role in the dynamics for $f_a \gtrsim 10^{16}$ GeV as typical of string axions [56].

Finally, we also did not consider more than one type of heavy ALP. This is because once the first superradiant instability occurs, the "Regge" trajectory should follow the superradiant threshold which means that we no longer intercept higher mass thresholds until very late, where superradiance stops being relevant.

To conclude, we showed that a primordial black hole which is evaporating today can be used to study signs of hidden dimensions predicted by string theory. The study of the black hole's dynamics and/or the cloud's dynamics allow for the calculation of not only the number of light ALP species in the universe, but also the mass of a heavy ALP which induces a superradiant instability. The future study of the photon flux and the consequences of the existence of these clouds will both improve our understanding of the universe, namely the physics beyond the Standard Model, and also the intrinsic nature of spacetime.

Bibliography

[1] Marco Calzà, John March-Russell, and João G. Rosa. *Evaporating primordial black holes, the string axiverse, and hot dark radiation*. 2021. DOI: 10.48550/ARXIV.2110.13602. URL: https://arxiv.org/abs/2110.13602.

[2] Roger Penrose and Wolfgang Rindler. *Spinors and Space-Time*. Vol. 1. Cambridge Monographs on Mathematical Physics. Cambridge University Press, 1984. DOI: 10.1017/CBO9780511564048.

[3] Inc. Wolfram Research. *Mathematica, Version 13.1*. Champaign, IL, 2022. URL: https://www.wolfram.com/mathematica.

[4] Robert M. Wald. *General relativity*. The University of Chicago Press, 1984.

[5] Roger Penrose. "Gravitational Collapse and Space-Time Singularities". In: 14.3 (Jan. 1965), pp. 57–59. DOI: 10.1103/PhysRevLett.14.57.

[6] Stephen Hawking and Ellis George F R. *The large scale structure of space-time*. Cambridge University Press, 1974.

[7] Robert H. Boyer and Richard W. Lindquist. "Maximal Analytic Extension of the Kerr Metric". In: *Journal of Mathematical Physics* 8.2 (Feb. 1967), pp. 265–281. DOI: 10.1063/1.1705193.

[8] Sean Carroll. *Spacetime and Geometry: An Introduction to General Relativity*. Pearson, 2003.

[9] E. Wigner. "On Unitary Representations of the Inhomogeneous Lorentz Group". In: *Annals of Mathematics* 40.1 (1939), pp. 149–204. ISSN: 0003486X. URL: http://www.jstor.org/stable/1968551 (visited on 07/29/2022).

[10] Steven Weinberg. *The quantum theory of Fields, Volume 1: Foundations*. Vol. 1. Cambridge Univ. Press, 1995.

[11] S. Chandrasekhar. *The mathematical theory of Black Holes*. Clarendon Press, 1998.

[12] J. N. Goldberg and R. K. Sachs. "A theorem on Petrov types". In: *Acta Physica Polonica B, Proceedings Supplement* 22 (Jan. 1962), p. 13.

[13] S. W. Hawking. "Gravitational Radiation from Colliding Black Holes". In: *Phys. Rev. Lett.* 26 (21 May 1971), pp. 1344–1346. DOI: 10.1103/PhysRevLett.26.1344. URL: https://link.aps.org/doi/10.1103/PhysRevLett.26.1344.

[14] Erik Curiel. "A Primer on Energy Conditions". In: *Towards a Theory of Spacetime Theories*. Springer New York, 2017, pp. 43–104. DOI: 10.1007/978-1-4939-3210-8_3. URL: https://doi.org/10.1007%2F978-1-4939-3210-8_3.

[15] S. W. Hawking. "Black holes in general relativity". In: *Communications in Mathematical Physics* 25.2 (1972), pp. 152–166. DOI: 10.1007/bf01877517.

[16] Jacob D. Bekenstein. "Generalized second law of thermodynamics in black-hole physics". In: *Phys. Rev. D* 9 (12 June 1974), pp. 3292–3300.

DOI: 10.1103/PhysRevD.9.3292. URL: https://link.aps.org/doi/10.1103/PhysRevD.9.3292.

[17] P. K. Townsend. *Black holes*. July 1997. URL: https://arxiv.org/abs/gr-qc/9707012.

[18] Istvá n Rácz and Robert M Wald. "Global extensions of spacetimes describing asymptotic final states of black holes". In: *Classical and Quantum Gravity* 13.3 (Mar. 1996), pp. 539–552. DOI: 10.1088/0264-9381/13/3/017. URL: https://doi.org/10.1088%2F0264-9381%2F13%2F3%2F017.

[19] Robert M. Wald. *Quantum field theory in curved spacetime and black hole thermodynamics*. The Universitiy of Chicago Press, 1994.

[20] Kerson Huang. *Statistical mechanics*. New York, 1987.

[21] Jacob D. Bekenstein. "Extraction of Energy and Charge from a Black Hole". In: *Phys. Rev. D* 7 (4 Feb. 1973), pp. 949–953. DOI: 10.1103/PhysRevD.7.949. URL: https://link.aps.org/doi/10.1103/PhysRevD.7.949.

[22] Don N. Page. *Particle emission rates from a black hole. II. massless particles from a rotating hole*. Dec. 1976. URL: https://journals.aps.org/prd/abstract/10.1103/PhysRevD.14.3260.

[23] Paulo B. Ferraz, Thomas W. Kephart, and João G. Rosa. "Superradiant pion clouds around primordial black holes". In: *Journal of Cosmology and Astroparticle Physics* 2022.07 (July 2022), p. 026. DOI: 10.1088/1475-7516/2022/07/026. URL: https://doi.org/10.1088%2F1475-7516%2F2022%2F07%2F026.

[24] Rodrigo Vicente, Vitor Cardoso, and Jorge C. Lopes. "Penrose process, superradiance, and ergoregion instabilities". In: *Physical Review D* 97.8 (Apr. 2018). DOI: 10.1103/physrevd.97.084032. URL: https://doi.org/10.1103%2Fphysrevd.97.084032.

[25] W. Unruh. "Separability of the Neutrino Equations in a Kerr Background". In: *Phys. Rev. Lett.* 31 (20 Nov. 1973), pp. 1265–1267. DOI: 10.1103/PhysRevLett.31.1265. URL: https://link.aps.org/doi/10.1103/PhysRevLett.31.1265.

[26] S. M. Wagh and N. Dadhich. "Absence of super-radiance of the Dirac particles in the Kerr-Newman geometry and the weak positive-energy condition". In: *Phys. Rev. D* 32 (8 Oct. 1985), pp. 1863–1865. DOI: 10.1103/PhysRevD.32.1863. URL: https://link.aps.org/doi/10.1103/PhysRevD.32.1863.

[27] S. W. Hawking. "Particle Creation by Black Holes". In: *Commun. Math. Phys.* 43 (1975). Ed. by G. W. Gibbons and S. W. Hawking. [Erratum: Commun.Math.Phys. 46, 206 (1976)], pp. 199–220. DOI: 10.1007/BF02345020.

[28] Robert M. Wald. "On Particle Creation by Black Holes". In: *Commun. Math. Phys.* 45 (1975), pp. 9–34. DOI: 10.1007/BF01609863.

[29] W. G. Unruh. "Notes on black-hole evaporation". In: *Phys. Rev. D* 14 (4 Aug. 1976), pp. 870–892. DOI: 10.1103/PhysRevD.14.870. URL: https://link.aps.org/doi/10.1103/PhysRevD.14.870.

[30] Bernard S. Kay and Robert M. Wald. "Theorems on the Uniqueness and Thermal Properties of Stationary, Nonsingular, Quasifree States on Space-Times with a Bifurcate Killing Horizon". In: *Phys. Rept.* 207 (1991), pp. 49–136. DOI: 10.1016/0370-1573(91)90015-E.

[31] Saul A. Teukolsky. "Perturbations of a Rotating Black Hole. I. Fundamental Equations for Gravitational, Electromagnetic, and Neutrino-Field Perturbations". In: 185 (Oct. 1973), pp. 635–648. DOI: 10.1086/152444.

[32] C. Flammer. *Spheroidal Wave Functions*. Standford University Press, 1957.

[33] Ian J.R. Aitchison and Anthony J.G. Hey. *Gauge theories in particle physics a practical introduction*. 4th. Vol. 2. CRC PRESS, 2012.

[34] Stephen Hawking. "Gravitationally collapsed objects of very low mass". In: 152 (Jan. 1971), p. 75. DOI: 10.1093/mnras/152.1.75.

[35] Bernard Carr and Florian Kühnel. "Primordial Black Holes as Dark Matter: Recent Developments". In: *Annual Review of Nuclear and Particle Science* 70.1 (2020), pp. 355–394. DOI: 10.1146/annurev-nucl-050520-125911.

[36] João Rosa. *Introduction to cosmology*. URL: http://gravitation.web.ua.pt/cosmo.

[37] Edward W. Kolb and Michael S. Turner. *The Early Universe*. Vol. 69. 1990. ISBN: 978-0-201-62674-2. DOI: 10.1201/9780429492860.

[38] Christian T. Byrnes and Philippa S. Cole. *Lecture notes on inflation and primordial black holes*. 2021. DOI: 10.48550/ARXIV.2112.05716. URL: https://arxiv.org/abs/2112.05716.

[39] V. De Luca et al. "The initial spin probability distribution of primordial black holes". In: *Journal of Cosmology and Astroparticle Physics* 2019.05 (May 2019), pp. 018–018. DOI: 10.1088/1475-7516/2019/05/018. URL: https://doi.org/10.1088%2F1475-7516%2F2019%2F05%2F018.

[40] Mehrdad Mirbabayi, Andrei Gruzinov, and Jorge Noreña. "Spin of primordial black holes". In: 2020.3, 017 (Mar. 2020), p. 017. DOI: 10.1088/1475-7516/2020/03/017. arXiv: 1901.05963 [astro-ph.CO].

[41] Takeshi Chiba and Shuichiro Yokoyama. "Spin distribution of primordial black holes". In: *Progress of Theoretical and Experimental Physics* 2017.8 (Aug. 2017). 083E01. ISSN: 2050-3911. DOI: 10.1093/ptep/ptx087. eprint: https://academic.oup.com/ptep/article-pdf/2017/8/083E01/19488901/ptx087.pdf. URL: https://doi.org/10.1093/ptep/ptx087.

[42] R. D. Peccei and Helen R. Quinn. "CP Conservation in the Presence of Pseudoparticles". In: *Phys. Rev. Lett.* 38 (25 June 1977), pp. 1440–1443. DOI: 10.1103/PhysRevLett.38.1440. URL: https://link.aps.org/doi/10.1103/PhysRevLett.38.1440.

[43] C. A. Baker et al. "Improved experimental limit on the electric dipole moment of the neutron". In: *Physical Review Letters* 97.13 (2006). DOI: 10.1103/physrevlett.97.131801.

[44] Th. Kaluza. "Zum Unitätsproblem der Physik". In: *Sitzungsber. Preuss. Akad. Wiss. Berlin (Math. Phys.)* 1921 (1921), pp. 966–972. DOI: 10.1142/S0218271818700017. arXiv: 1803.08616 [physics.hist-ph].

[45] Oskar Klein. "Quantum Theory and Five-Dimensional Theory of Relativity. (In German and English)". In: *Z. Phys.* 37 (1926). Ed. by J. C. Taylor, pp. 895–906. DOI: 10.1007/BF01397481.

[46] Asimina Arvanitaki et al. "String axiverse". In: *Physical Review D* 81.12 (June 2010). DOI: 10.1103/physrevd.81.123530. URL: https://doi.org/10.1103%2Fphysrevd.81.123530.

[47] Michael R. Douglas and Shamit Kachru. "Flux compactification". In: *Reviews of Modern Physics* 79.2 (May 2007), pp. 733–796. DOI: 10.1103/revmodphys.79.733. URL: https://doi.org/10.1103%2Frevmodphys.79.733.

[48] Peter Svrcek and Edward Witten. "Axions in string theory". In: *Journal of High Energy Physics* 2006.06 (June 2006), pp. 051–051. DOI: 10.1088/1126-6708/2006/06/051. URL: https://doi.org/10.1088%2F1126-6708%2F2006%2F06%2F051.

[49] Edward Witten. "Dynamical Breaking of Supersymmetry". In: *Nucl. Phys. B* 188 (1981), p. 513. DOI: 10.1016/0550-3213(81)90006-7.

[50] Edward Witten. "Some properties of O(32) superstrings". In: *Physics Letters B* 149.4 (1984), pp. 351–356. ISSN: 0370-2693. DOI: https://doi.org/10.1016/0370-2693(84)90422-2. URL: https://www.sciencedirect.com/science/article/pii/0370269384904222.

[51] Brett E. Taylor, Chris M. Chambers, and William A. Hiscock. "Evaporation of a Kerr black hole by emission of scalar and higher spin particles". In: *Physical Review D* 58.4 (July 1998). DOI: 10.1103/physrevd.58.044012. URL: https://doi.org/10.1103%2Fphysrevd.58.044012.

[52] Chris M. Chambers, William A. Hiscock, and Brett Taylor. *Spinning down a black hole with scalar fields*. Mar. 1997. URL: https://arxiv.org/abs/gr-qc/9703018.

[53] John March-Russell and João G. Rosa. "Micro-Bose/Proca dark matter stars from black hole superradiance". In: (May 2022). arXiv: 2205.15277 [gr-qc].

[54] R. L. Workman et al. "Review of Particle Physics". In: *PTEP* 2022 (2022), p. 083C01. DOI: 10.1093/ptep/ptac097.

[55] J. H. MacGibbon and B. R. Webber. "Quark and gluon jet emission from primordial black holes: The instantaneous spectra". In: *Phys. Rev. D* 41 (1990), pp. 3052–3079. DOI: 10.1103/PhysRevD.41.3052.

[56] Masha Baryakhtar et al. "Black hole superradiance of self-interacting scalar fields". In: *Physical Review D* 103.9 (May 2021). DOI: 10.1103/physrevd.103.095019. URL: https://doi.org/10.1103%2Fphysrevd.103.095019.